Available online at www.sciencedirect.com
SCIENCE DIRECT
Coordination Chemistry Reviews 250 (2006) 388–413
COORDINATION CHEMISTRY REVIEWS
www.elsevier.com/locate/ccr

Review

Annual review of organometallic and nitrosyl photochemistry: 2003

Thomas E. Bitterwolf *

Department of Chemistry, University of Idaho, Moscow, ID 83844-2343, United States

Received 2 March 2005; accepted 19 October 2005
Available online 28 December 2005

Contents

Abstract

The literature of organometallic and nitrosyl photochemistry for 2003 has been reviewed.

Keywords: Organometallic; Nitrosyl; Photochemistry

Photochemistry has played a significant role in transition metal organometallic chemistry since its emergence as a discipline in the early 1900s. Early studies took advantage of the selective exchange of carbonyl ligands upon photolysis, while more recent work has examined ligand rearrangements, metal–metal bond breaking, a variety of charge transfer processes and the creation of intermediates that may serve as catalysts in subsequent reactions. A variety of high speed methods, notably time-resolved IR spectroscopy and time-resolved resonance Raman spectroscopy have made possible the examination of excited state species within picoseconds of their formation, and to follow the evolution of these species and their reactions. These studies have shed light on the mechanisms of photochemical and thermal reactions as it is not unusual for the same intermediates to be involved in both processes. In recognition of the steady progress in this field, an invitation was recently extended to initiate a series of annual reviews summarizing the developments. By beginning with 2003, this review overlaps slightly with a comprehensive review of the photochemistry of organometallic and related compounds (for example, metal nitrosyl compounds) covering the years 1992–2002 recently published in the Encyclopaedia of Inorganic Chemistry [1] and a historical overview of organometallic photochemistry prepared as part of the 40th Anniversary of the Journal of Organometallic Chemistry [2].

1. Synthetic applications of photochemistry

As might be expected, the largest class of reactions reported in 2003 involves the photochemical loss of CO to yield reactive intermediates that subsequently add two electron donor ligands, such as phosphines or undergo oxidative addition with a variety of substrates.

Darensbourg et al., have photolyzed $[CpFe(CN)_2CO]^{1-}$ in the presence of phosphines and diphosphines to yield $[CpFe(CN)_2PR_3]^{1-}$ and $\{[CpFe(CN)_2]_2(\mu\text{-}R_2P(CH_2)_nPR_2)\}^{2-}$ derivatives [3]. The phosphine derivatives were subsequently reacted with Cu(I) yielding cyclic species in which CN groups bridged iron and Cu(I) centers. An example of these cyclic species is illustrated in Fig. 1.

Şentürk and co-workers reported several reactions involving the photolysis of transition metal carbonyl compounds with a variety of nitrogen and sulfur ligands. For example, the methyl [4] and ethyl [5] derivatives of 2-

* Tel.: +1 208 885 6361; fax: +1 208 885 6173.
E-mail address: bitterte@uidaho.edu.

0010-8545/$ – see front matter © 2005 Elsevier B.V. All rights reserved.
doi:10.1016/j.ccr.2005.10.019

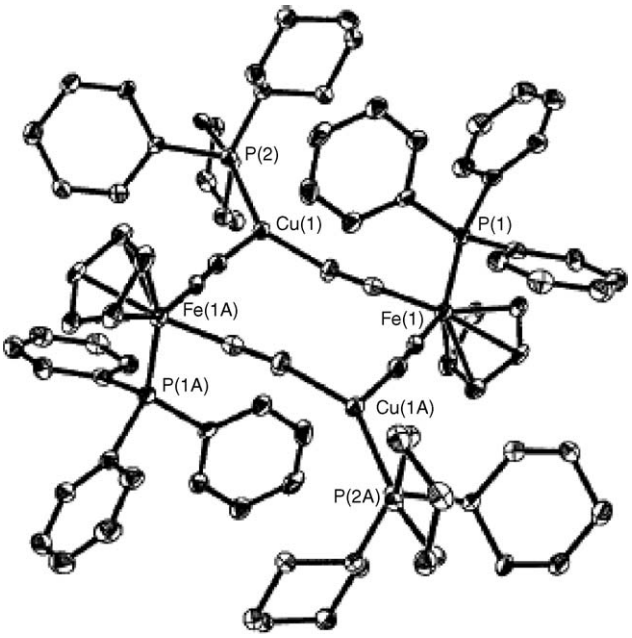

Fig. 1. Thermal ellipsoid representation of $[CpFe(PPh_3)(\mu\text{-}CN)_2CuPCy_3]_2$ with hydrogens removed for clarity (Ref. [3]).

hydroxyacetophenonesulfonylhydrazone (apmsh and apesh), Ia and Ib, react with $M(CO)_6$, M = Cr, Mo, W and $Re(CO)_5Br$ photochemically to yield CO-loss derivatives. It is proposed on the basis of C=N stretching frequency shifts that the ligand is bound through the imine nitrogen, e.g. $Mo(CO)_5$(apmsh), II. Interestingly, with $CpMn(CO)_3$ the cyclopentadienyl ligand is displaced to give an $Mn(CO)_3$ derivative in which it is proposed that the apmsh ligand is bound through both of the nitrogens and the phenoxide group, III.

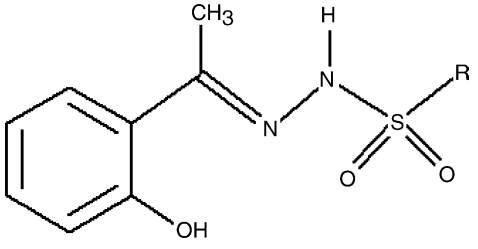

Ia, R =Me

Ib, R =Et

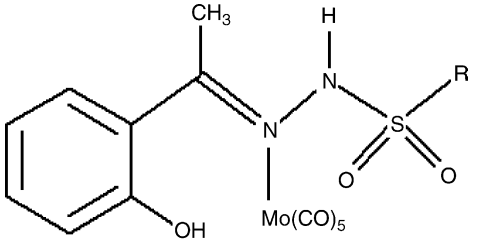

II

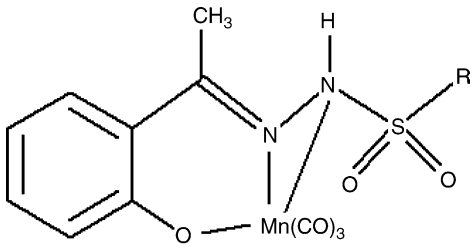

III

Photolysis of the group VI carbonyls, $Re(CO)_5Br$ and $CpMn(CO)_3$ with the pesticide 3,5-dimethyl-tetrahydro-2H-1,3,5 thiadiazine-2-thione (DTTT), IV, leads to simple substitution products, such as $W(CO)_5$(DTTT), Fig. 2 [6]. $Re(CO)_5Br$ reacts photochemically with tetraalkyldiphosphinedisulfides, $R_2P(S)P(S)R_2$, where R = Me, Et, Pr, Bu, Ph, to give chelated *fac*-$Re(CO)_3(\eta^2\text{-}R_2P(S)P(S)R_2$ derivatives or bimetallic species in which the diphosphine is believed to substitute in a cis orientation. The molecular structure of *fac*-$Re(CO)_3Br(\eta^2\text{-}Et_2P(S)P(S)Et_2)$ is shown in Fig. 3 [7].

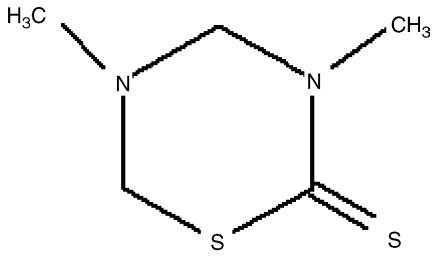

IV

Mathur et al. have applied photochemistry to the reactions of $Fe_3(CO)_9(\mu^3\text{-}S)_2$, $CpMo(CO)_3$ (acetylide) and a terminal acetylene or ferrocenylacetylene [8]. These workers had carried out earlier studies on the thermolysis of $Fe_3(CO)_9(\mu^3\text{-}S)_2$

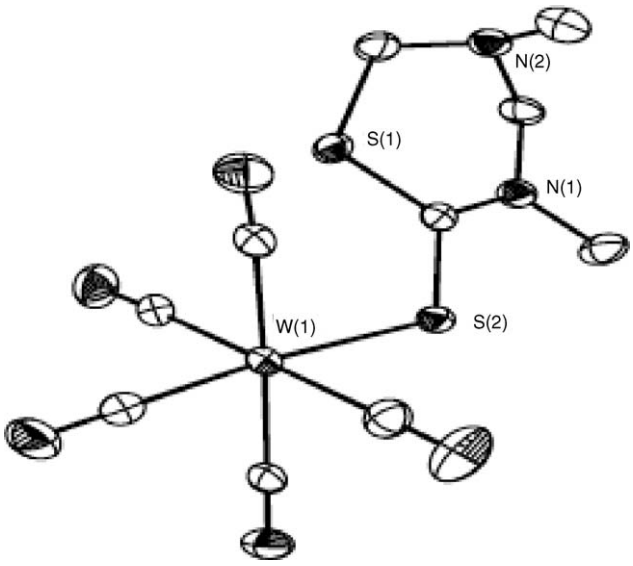

Fig. 2. Molecular structure of $W(CO)_5$(DTTT) (Ref. [6]).

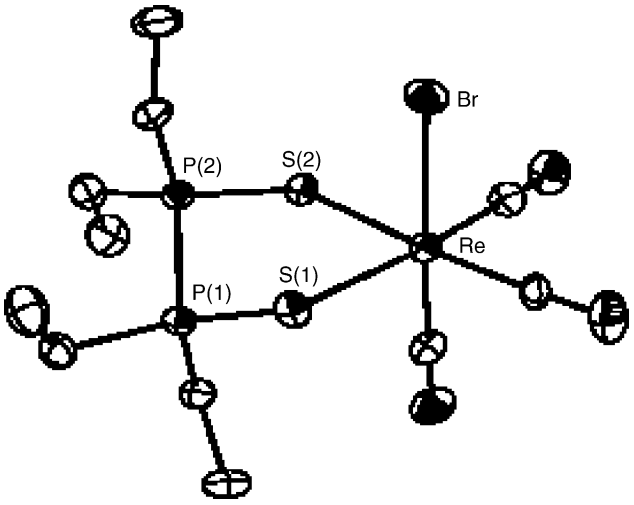

Fig. 3. Molecular structure of *fac*-$Re(CO)_3Br(\eta^2\text{-}Et_2P(S)P(S)Et_2)$ (Ref. [7]).

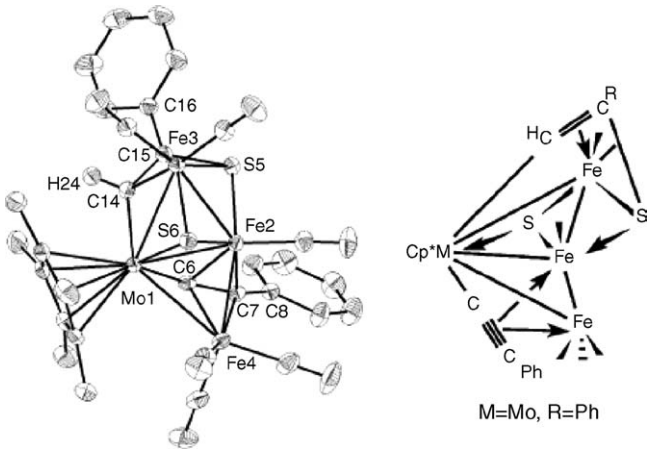

Fig. 4. Molecular structure of $[Cp^*MoFe_3(\mu^3\text{-}S)\{\mu^3\text{-}C(H)=C(Ph)S\}(CO)_6(\mu^3CCPh)]$ with connectivity diagram (Ref. [8]).

and $CpM(CO)_3$ (acetylide), where M = Mo or W [9]. Complex cluster species such as that shown in Fig. 4 are produced. As there are several possible sites for metal carbonyl loss it is not clear which of the several species loses CO to initiate the cluster formation.

Godoy et al. have examined the thermal reductive elimination of C_6HF_5 from $(\eta^5\text{-}C_5Me_4R)Re(CO)_2(H)(C_6F_5)$, where $R=(CH_2)_2CH=CH_2$ and $CH_2\text{–}2\text{–}C_4H_3S$ with the goal of observing products in which the pendant olefin and thienyl groups form chelate rings with the rhenium metal [10]. In the absence of an overpressure of CO extensive decomposition took place although IR bands consistent with the anticipated chelated species were observed. When $[\eta^5\text{-}C_5Me_4(CH_2\text{–}2\text{–}C_4H_3S)]Re(CO)_3$ was photolyzed in hexane the desired chelated species, V, was isolated in small yield.

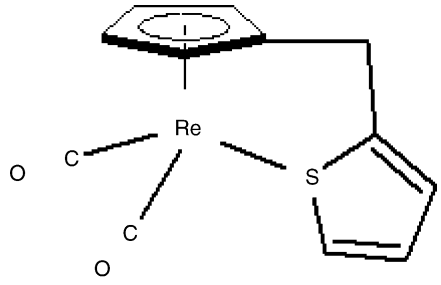

V

Photochemical loss of ethene has also been reported. Photolysis of $CpRh(C_2H_4)_2$ in the presence of 2-vinylpyridine results in substitution of the ethylene ligands by one or two vinyl bound 2-vinylpyridine ligands [11]. Interestingly, while no N-bound pyridine mononuclear species were isolated, a small amount of $(CpRh)_2(\mu\text{-}\eta^1, \eta^2\text{-}CH_2=CH\text{–}Py)_2$ was recovered. Finally, a bimetallic species resulting from insertion of Rh into a C-H bond of the terminal vinyl CH_2, Fig. 5, was isolated.

A substantial literature exists examining the photochemistry of Fp-silyl (Fp = $CpFe(CO)_2$) derivatives, particularly the rearrangement of oligiosilyl groups via the intermediacy of silene-iron species. The thermal or photochemical loss of a carbon monoxide ligand opens a coordination site on the metal facilitating α-eliminations. The resulting species undergo complex equilibria involving 1,3 alkyl, aryl and silyl rearrangements. Three papers by the Pannell group and a fourth by Okazaki and co-workers have examined the rearrangement of oligiosilane and silyl-tellurium groups, respectively.

Photolysis of Fp-disilane derivatives generally results in formation of a Fp-monosilane product with loss of a silylene group. In order to better understand the nature of the 1,3 rearrangements, Pannell and Zhang prepared a set of three isomeric Fp-disilane derivatives, VI–VIII, and examined their photoproducts [12]. Despite their apparent structural differences, the three compounds yielded $FpSiMe_3$ and $FpSi(Me)(CH_2)_4$, IX, in equivalent ratios. To explain these

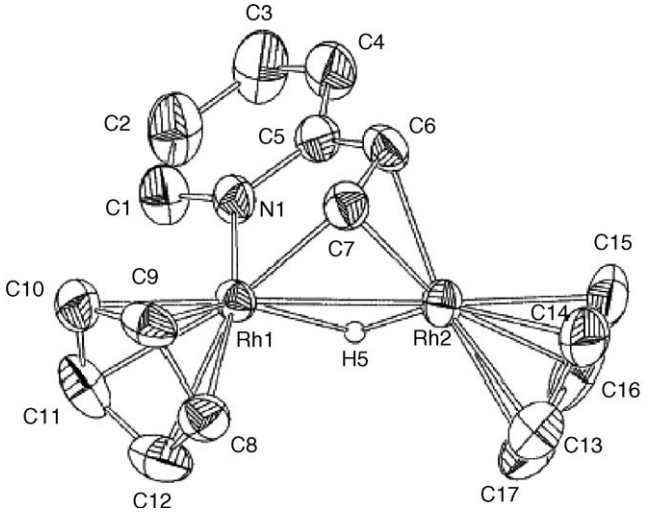

Fig. 5. Molecular structure of $(CpRh)_2(\mu\text{-}H)(\mu\text{-}\eta^1, \eta^1, \eta^2\text{-}CH=CH\text{-}Py)$ (Ref. [11]).

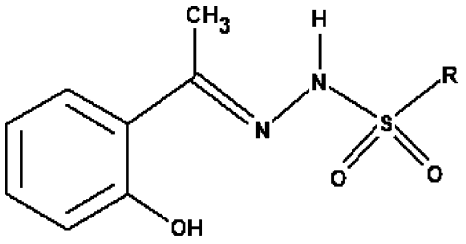

Ia, R = Me

Ib, R = Et

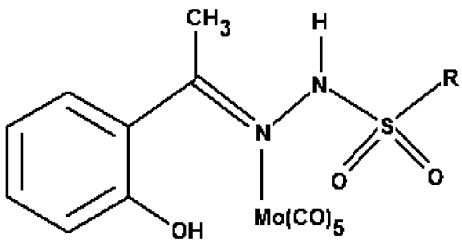

II

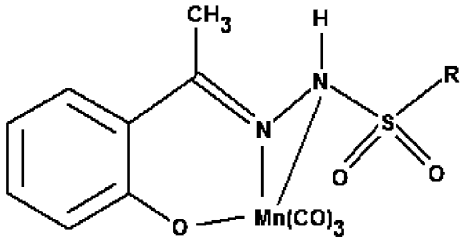

III

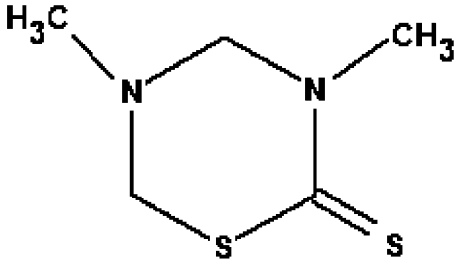

IV

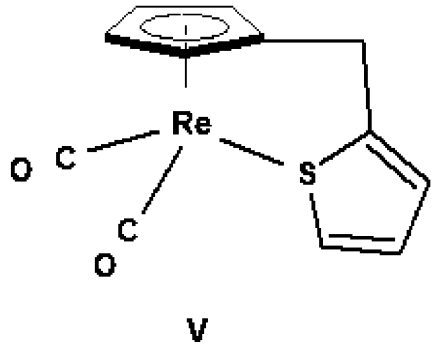

V

Scheme 1. (Ref. [12]).

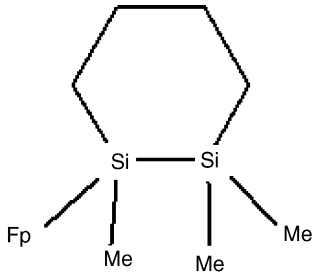

VI

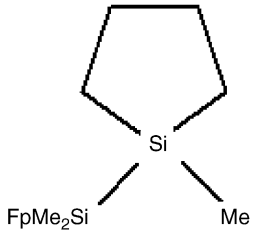

VII

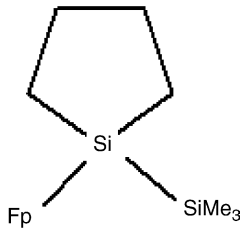

VIII

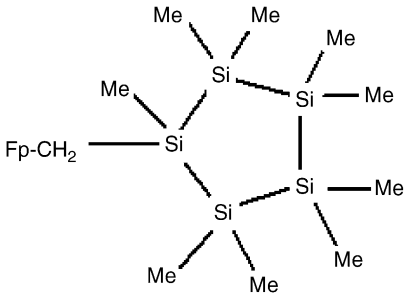

X

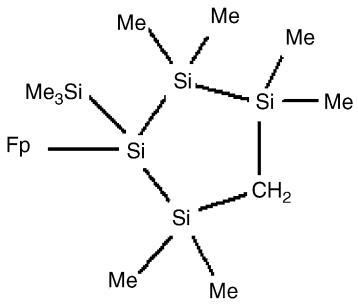

XI

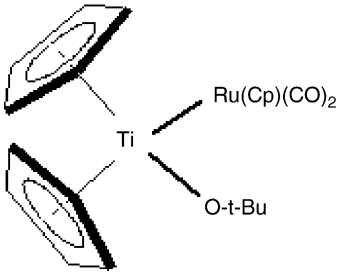

XVI

Scheme 1. (*Continued*)

observations the intermediates illustrated in Scheme 1 have been proposed.

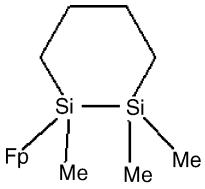

VI

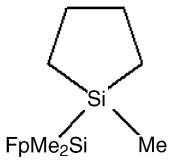

VII

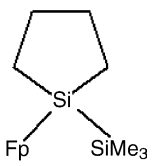

VIII

The cyclopentylsilane derivative, X, has been prepared and its photochemistry examined [13]. A single product, XI, was formed in high yield with no evidence of intermediates. It is proposed that a complex series of α- and β-rearrangements may account for the observed transformation. Photolysis of the bimetallic derivatives, XII and XIII result in the series of products illustrated in Schemes 2 and 3 (only one of several isomeric species is illustrated) [14].

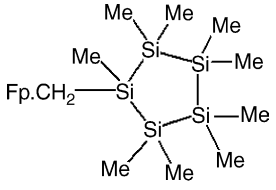

X

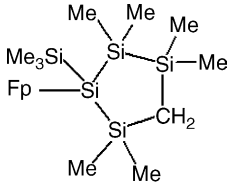

XI

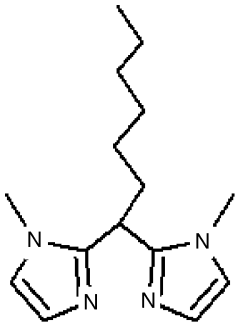

XVII

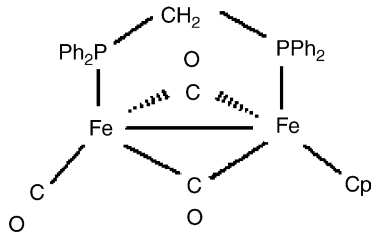

XVIII

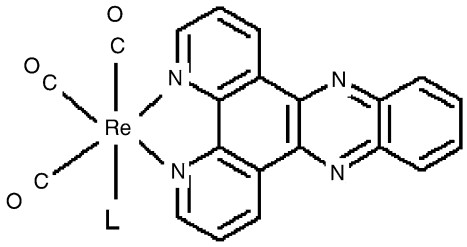

XIX: L = Py

XX: L = Cl

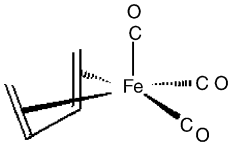

XXI

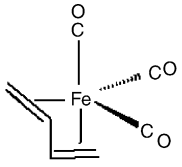

XXII

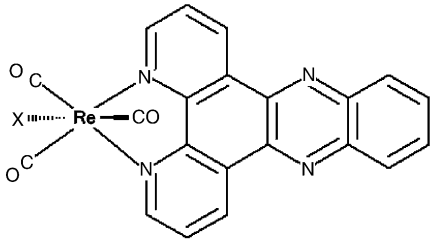

X = py or Cl

XXIII

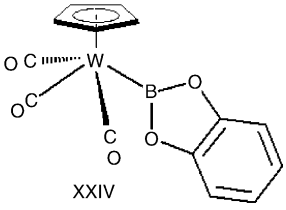

XXIV

Scheme 1. (*Continued*)

Closely related to the polysilane studies described above is the examination of the photolysis of $FpSi(Me)_2TePh$, XIV, by Okazaki and co-workers [15]. Photolysis in the presence of acetone as a trap for the photochemical intermediates results in formation of a tellurasilacycle, XV. The molecular structures of XIV and XV are shown in Fig. 6a and b. The reaction is proposed to proceed through capture of the intermediate shown in Scheme 4.

A very effective strategy for enhancing the efficiency of chemical reactions is to design intermediates so that reductive elimination of methane or similar small molecules harnesses an entropic driving force. An example of this effect has been reported by Okazaki et al. in the photochemical synthesis of Fp-silane compounds [16]. Conventional synthetic routes involve reaction of the Fp anion with an appropriate silane halide as shown in Scheme 5a. Alternatively, photolysis of Fp-Me in the presence of a substituted silane as shown in Scheme 5b combines an oxidative addition of the silane to the unsaturated CpFe(CO)Me species followed by reductive elimination of methane and recapture of CO to yield the product. In the particular case shown in Scheme 5, the desired product could not be separated from byproducts using the Fp anion, but was isolated in 48% yield from the photochemical route.

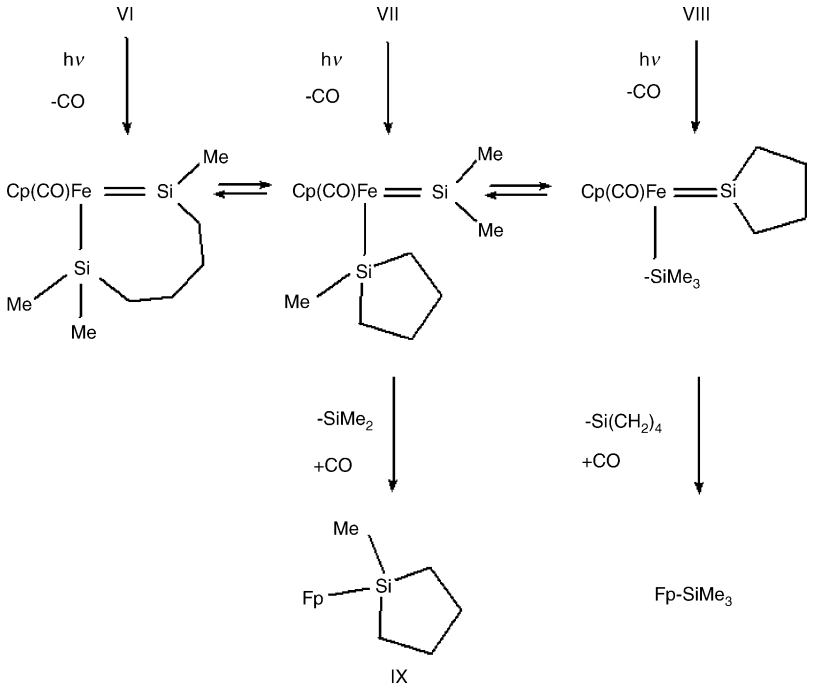

Scheme 1. (*Continued*).

Photolysis of metal cis-dihydrides frequently leads to reductive elimination of H_2 and formation of a highly reactive unsaturated metal center. Parkin et al. have reported the photolysis of $(\eta^5\text{-}C_5H_4CMe_3)_2MoH_2$ and isolation of *trans*-$[(\eta^5\text{-}C_5H_4CMe_3)Mo(\mu\text{-}\eta^1, \eta^5\text{-}C_5H_3CMe_3)H]_2$, Fig. 7 [17].

As part of a continuing investigation of the reactions of organometallic species with fullerenes, Baird and co-workers [18] have examined the reactions of various organometallic anions with C_{60}. C_{60} has a low lying triply degenerate LUMO that readily accepts electrons from metal anions. In the current investigation, $[CpFe(CO)_2]$, $[CpMo(CO)_3]$ and $[CpW(CO)_3]$ have been found to undergo electron transfer reactions with C_{60} to yield C_{60} and the respective radicals. Radical recombination is faster than reaction with the C_{60}, thus the bimetallic dimers are found to be the dominant metal products of the reaction. Reasoning that photolysis could generate a steady state concentration of

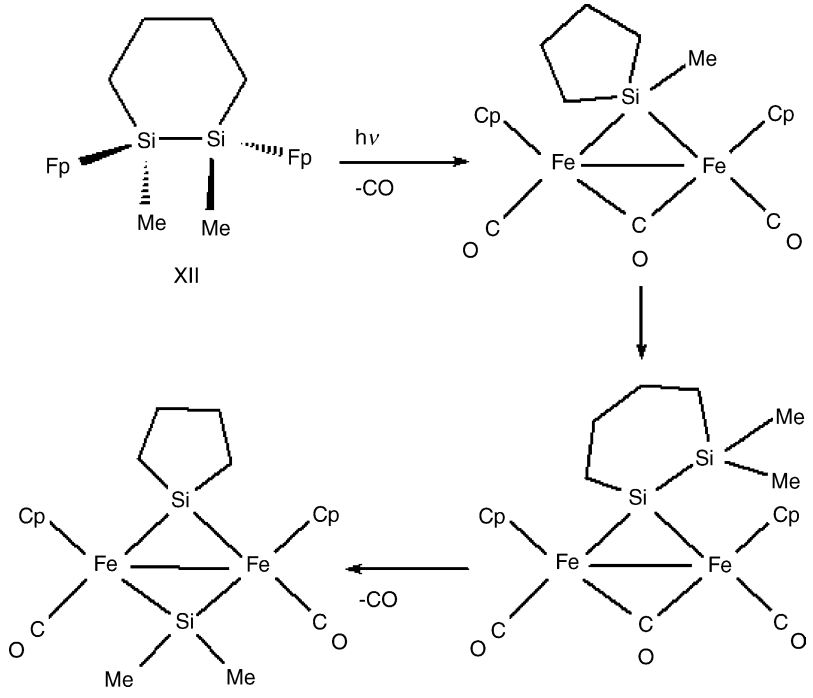

Scheme 2. (Ref. [14]).

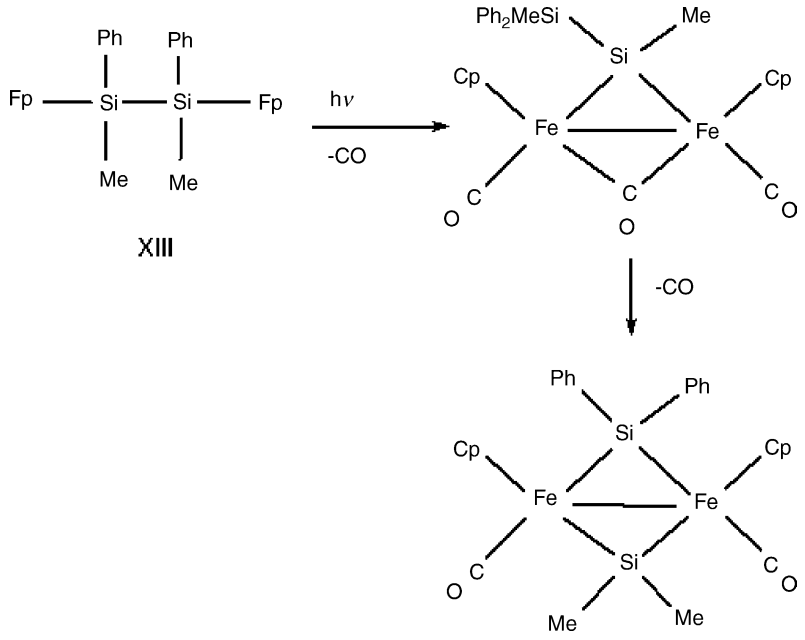

Scheme 3. (Ref. [14]).

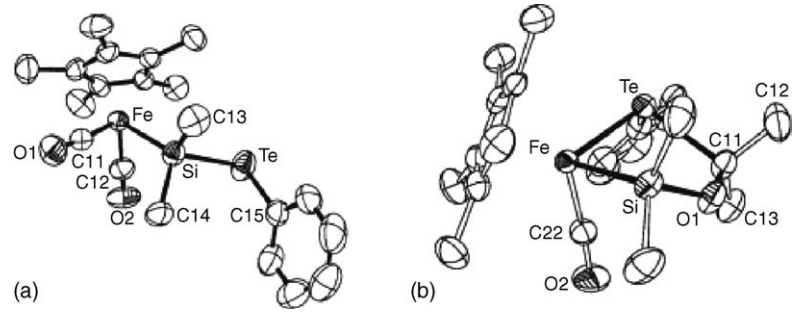

Fig. 6. Molecular structures of (a) XIV and (b) XV (Ref. [15]).

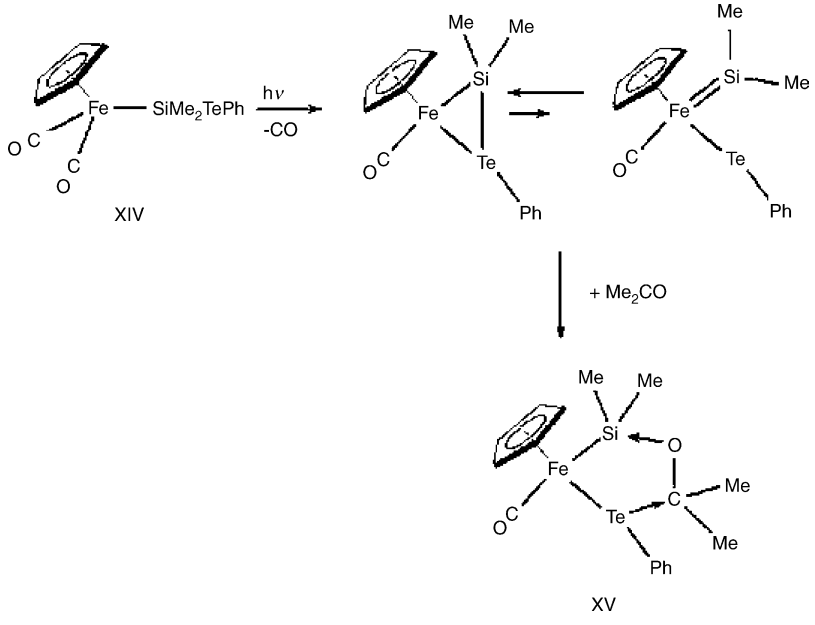

Scheme 4. (Ref. [15]).

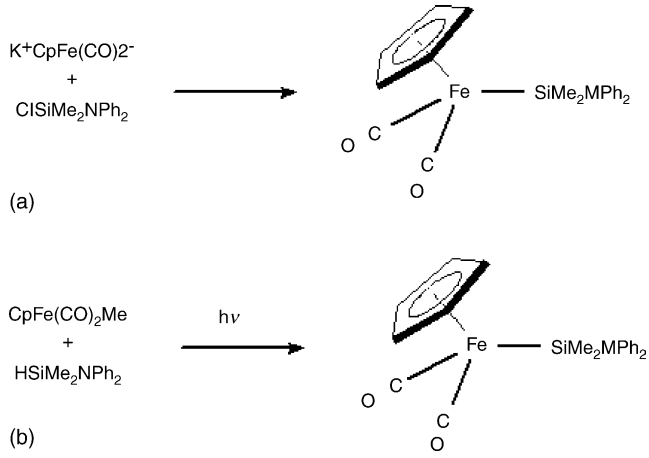

Scheme 5. (Ref. [16]).

radicals, thus increasing the probability of radical reaction with the fulleride anion, the reactions were repeated under photolysis conditions. No additional reaction was observed between the $CpFe(CO)_2$ radicals and the fulleride anion, but products corresponding to $[C_{60}CpM(CO)_2]$ were isolated for M = Mo and W. The compounds are proposed to bind to the fulleride in an η^2 manner as shown in Fig. 8.

Matsubara et al. have examined the reactions of the unique Ti(III) metallocene, $Cp_2Ti(O\text{-}t\text{-}Bu)$ with $[CpM(CO)_3]_2$, where M = Mo and W, and $[CpRu(CO)_2]_2$ [19]. The group VI compounds reacted thermally to form species with a bridging isocarbonyl linkage, while the ruthenium dimer reacted photochemically to yield XVI having a direct Ti–Ru bond. Curiously, this species underwent dissociation in the dark with reformation of the starting materials suggesting that the Ti–Ru bond is highly strained.

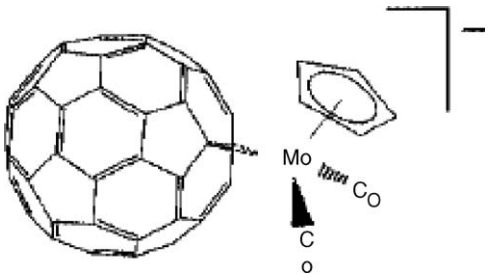

Fig. 8. Proposed structure of $[C_{60}CpMo(CO)_3]$ (Ref. [18]).

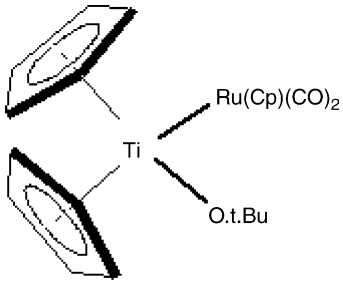

XVI

Photochemically generated $W(CO)_5(THF)$ has been found to be an effective catalyst for the electrophilic activation of allenyl groups for attack by carbon nucleophiles. Lee and co-workers [20] have reported the use of $W(CO)_6$ as a photocatalyst to effect the closure of rings where an allene group is adjacent to a carbon nucleophile. The proposed mechanism of this reaction is presented in Scheme 6. Similar reactions may also be achieved with terminal acetylene groups.

$W(CO)_5(THF)$ has also been found to be an effective catalyst in the cycloisomerization of alkynols. Wipf and Graham [21] have found that temperature, Scheme 7 and substituent orientation, Scheme 8, play a role in determining the product distribution of these reactions. They propose a mechanism in which an initially formed η^2-alkyne complex may close to form a five atom ring, while rearrangement of this species to a vinylidene results in closure to a six atom ring.

Photolysis of $(\eta^5\text{-}C_5Me_5)Re(CO)_3$ in the presence of chlorinated hydrocarbons results in the oxidative addition of an arene-Cl bond to the $(\eta^5\text{-}C_5Me_5)Re(CO)_2$ photofragment. Klahn and co-workers have examined this reaction with 2,4,5-trichloroanisole and 3,4,5-trichlorotrifluoromethylbenzene as substrates and isolated single products in each case [22]. The anisol compound undergoes oxidative addition exclusively at the 2-chloro, while the trifluoromethylbenzene undergoes addition at the 3-chloro. The molecular structure of the anisol derivative is presented in Fig. 9.

Photolysis of TpRh(1,5-COD), where COD, cyclooctadiene, at 400 nm by Traverso and co-workers [23] initiated rearrangement of the COD ligand to its conjugated 1,3-isomer. Photolysis

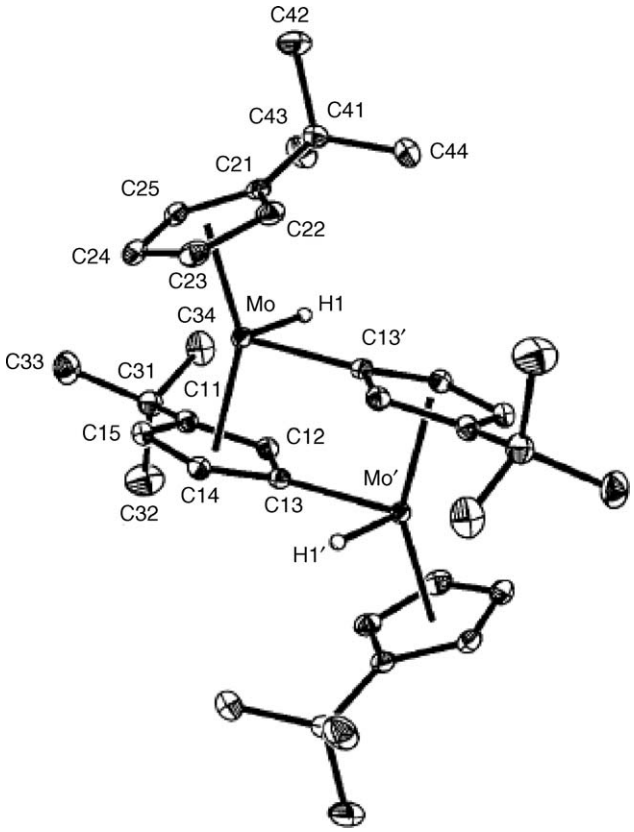

Fig. 7. Molecular structure of *trans*-$[(\eta^5\text{-}C_5H_4CMe_3)Mo(\mu\text{-}\eta^1, \eta^5\text{-}C_5H_3CMe_3)H]_2$ (Ref. [17]).

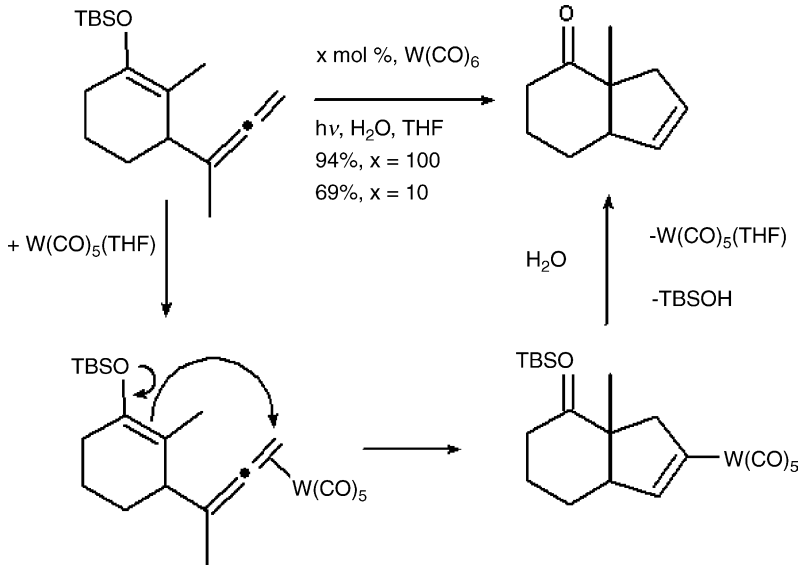

Scheme 6. (Ref. [20]).

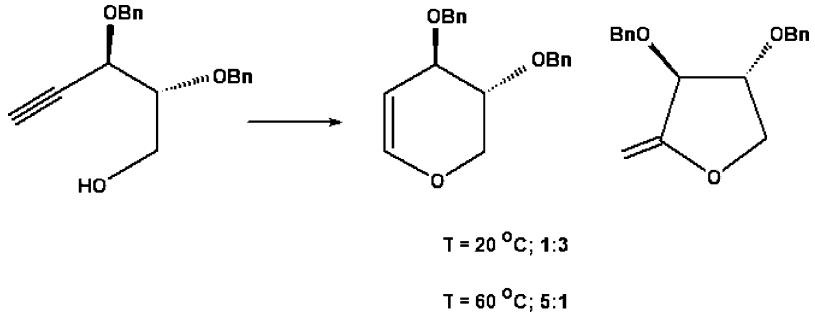

Scheme 7. (Ref. [21]).

of this species at higher energy (336 nm) resulted in loss of the 1,3-COD ligand with proposed formation of a "TpRh" fragment. When this latter photolysis was carried out in benzene in the presence of trimethylphosphite, TpRh(Ph)(H)([P(OMe)$_3$]) was isolated from the reaction. Substitution of *t*-butyl acrylate for the phosphite gave the chelated species, TpRh(Ph)($CH_2CH_2CO_2$-*t*-Bu). The order of benzene oxidative addition and phosphite or acrylate addition is not yet known. Photolysis of TpRh(1,3-COD) in methanol results in the formation of TpRh(H)$_2$(CO). The authors propose a sequence of hydrogen transfers from methanol to the rhodium resulting in complete dehydration of the methanol yielding a carbon monoxide ligand.

Burns et al. [24] have prepared the neutral bis(imidazole) ligand, (hexyl)CH(mim)$_2$ XVII and allowed this ligand to react with Pd(COD)Cl_2 or Pd(COD)(Cl)Me to yield palladium complexes. The molecular structure of the (hexyl)CH(mim)$_2$PdCl$_2$

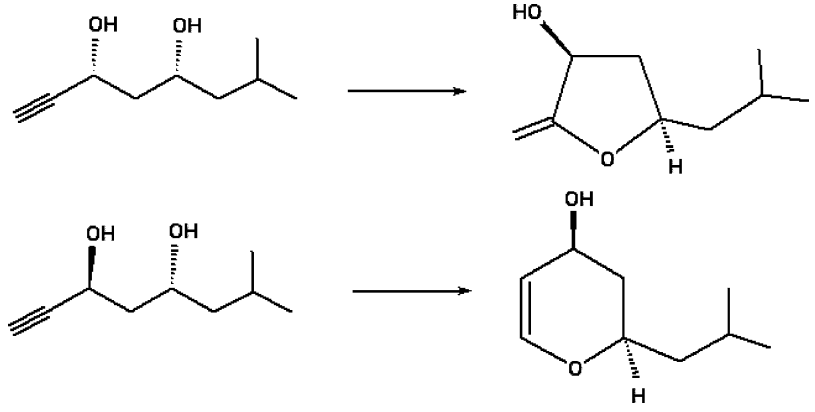

Scheme 8. (Ref. [21]).

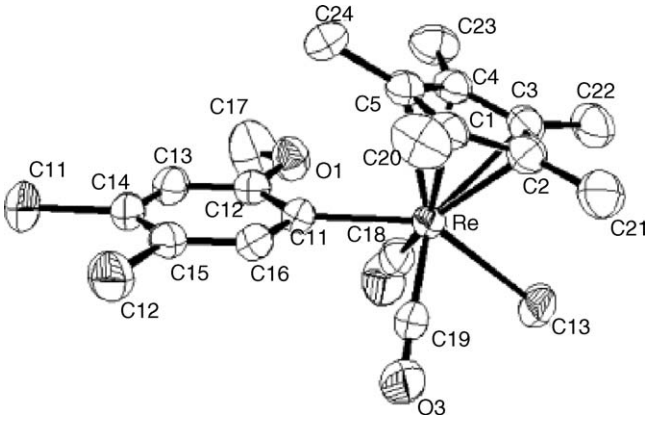

Fig. 9. Molecular structure of *trans*-(η^5-C_5Me_5)Re(CO)$_2$ [$C_6H_2Cl_2$(OMe)]Cl (Ref. [22]).

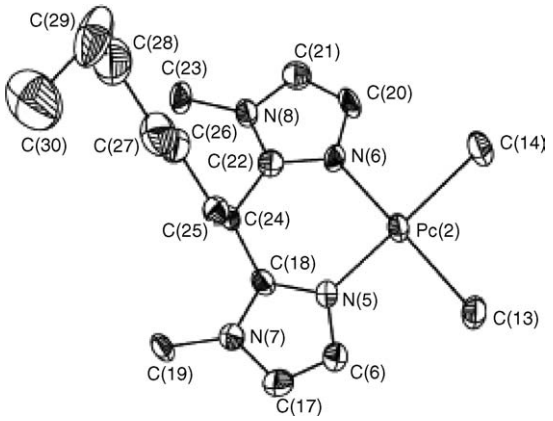

Fig. 10. Molecular structure of (hexyl)HC(mim)$_2$PdCl$_2$ (Ref. [24]).

is presented in Fig. 10. Ambient light results in the photolysis of (hexyl)CH(mim)$_2$Pd(Cl)Me in CH_2Cl_2 with formation of (hexyl)CH(mim)$_2$Pd(Cl)($CHCl_2$). Labeling experiments have provided strong evidence that the Pd–Me bond undergoes photochemical homolysis, followed by methyl radical abstraction of a hydrogen from CH_2Cl_2 and subsequent capture of the $CHCl_2$ radical by Pd.

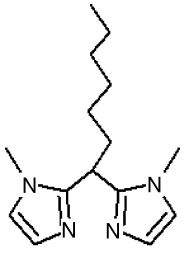

XVII

Some years ago it was established that $Cp_2Fe_2(\mu\text{-}CO)_2(\mu\text{-}\eta^2\text{-dppm})$, XVIII, was inert to photolysis [25]. In contrast, Ruiz and co-workers [26] have found that photolysis of $Cp_2Fe_2(CO)_4$ with dppm yields a complex potpourri of compounds, Scheme 9, many of which arise from iron insertion into C–H or P–C bonds. A number of mechanisms are presented to account for the products involving radicals and oxidative insertions leading to highly twisted intermediates. Of particular interest are the

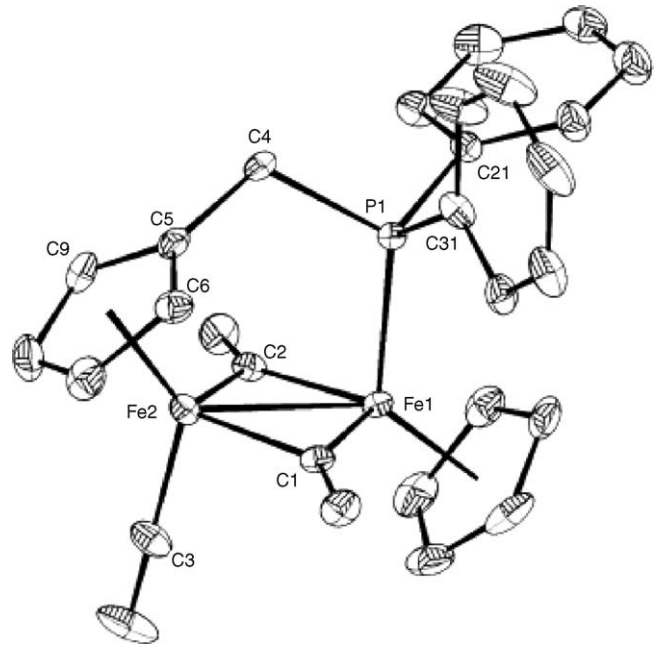

Fig. 11. Molecular structure of (μ-η^5, η^1-$C_5H_4CH_2PPh_2$) (η^5-C_5H_5) $Fe_2(CO)(\mu\text{-}CO)_2$ (Ref. [25]).

reaction products in which a CH_2PPh_2 group has been added to a cyclopentadienyl ring. The molecular structure of one of these compounds is presented in Fig. 11.

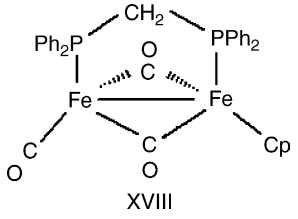

XVIII

2. Reaction mechanisms, theory and methods

For many years the Nottingham School has been at the forefront of developments in time-resolved IR methods as applied to photochemical problems. George and co-workers have reviewed these methods and their application to the study of molecular excited states and the direct observation of transient organometallic species [27].

In a related development, a team from the CCLRC Rutherford Appleton Laboratory, the University of Nottingham, and Imperial College have reported the addition of a broadband, picosecond infrared spectrometer to an existing ultrafast time-resolved resonance Raman, UV/visible and fluorescence spectrometer [28]. A schematic for the new infrared spectrometer is presented in Fig. 12. The infrared spectrometer is capable of recording broadband (ca. 150 cm^{-1} FWHM) using a set of 64 element MCT array detectors. As an illustration of the application of this new spectrometer to chemical problems, the spectrum of the excited state of two rhenium carbonyl dipyrido [3,2-*a*: 2′,3′]phenazine (dppz) derivatives were examined. The change in frequency of the carbonyl vibrations in these compounds are a probe for the shifts in electron density in the excited states.

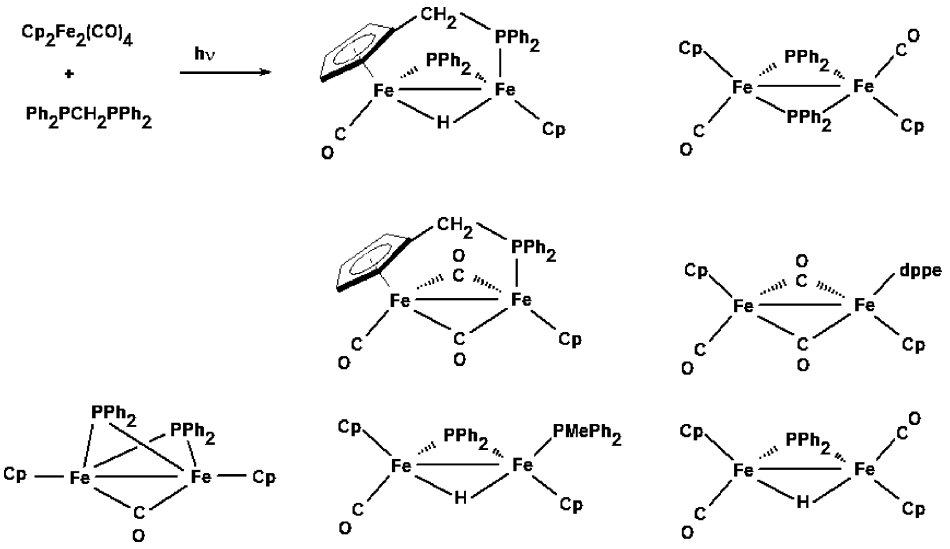

Scheme 9. Observed products from the reaction of Fp_2 with DPPM (Ref. [26]).

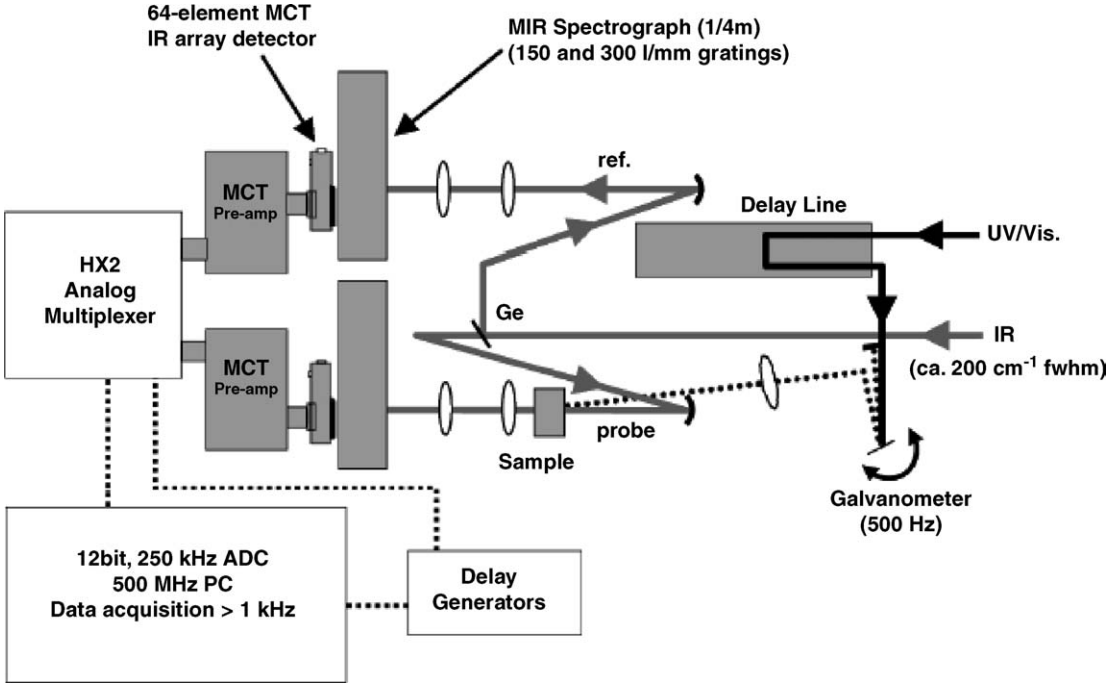

Fig. 12. Schematic diagram of broad band picosecond IR spectrometer (Ref. [28]).

As seen in Fig. 13a, photolysis of *fac*-$[Re(CO)_3(dppz)py]^{1+}$, XIX, results in bleaching of bands of the compound and appearance of two new bands at lower frequency. This work has been reported in some detail [29]. In contrast, photolysis of *fac*-$Re(CO)_3(dppz)Cl$, XX, Fig. 13b, results in carbonyl bands of the excited state shifting to higher frequency. In the former case it is proposed that dppz centered $\pi \rightarrow \pi^*$ transitions populate the ligand antibonding orbitals that are slightly better electron donors to the metal than the bonding π orbitals. In the latter case, a MLCT transition increases the effective charge on the Re, thus serving to withdraw electron density from the CO back bonding orbitals increasing the frequency of those vibrations. It should be noted that these spectra were recorded 100 ps after excitation.

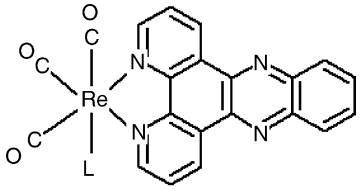

XIX: L = Py

XX: L = Cl

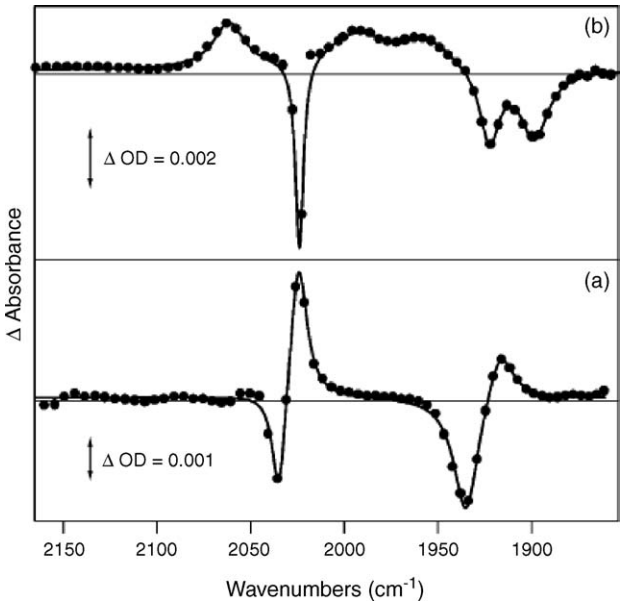

Fig. 13. TRIR spectra of (a) *fac*-[Re(CO)$_3$(dppz)Py] PF$_6$ in acetonitrile and (b) *fac*-Re(CO)$_3$(dppz)Cl in CH_2Cl_2, both recorded 100 ps after the 400 nm excitation. Both spectra are recorded at a spectral resolution of 8 cm^{-1} (Refs. [28] and [29]).

Time resolved IR methods have been applied to the characterization of noble gas compounds in supercritical Xe and Kr, and to the measurement of the rates of reaction between these species and CO [30]. In contrast to the behavior of CpM(CO)$_2$L and Cp*M(CO)$_2$L, where M = Mn or Re and L = Kr or Xe, for which rates of reaction with CO were unaffected by methyl substitution on the cyclopentadienyl ring, the rhodium compounds show a marked sensitivity to substitution. Following a trend observed for alkane complexes, pentamethylcyclopentadienyl derivatives were found to react more rapidly with CO than cyclopentadienyl derivatives [31]. Steric factors associated with the bulkier substituted ring were cited as the reason for the increased rates. A summary of the rates of noble gas complexes Cp′M(CO)$_n$L and M(CO)$_5$L with CO is presented in Fig. 14.

Time resolved IR spectroscopy has also been employed in the study of the photolysis of (η^4-*cis*-1,3-C_4H_6)Fe(CO)$_3$ XXI [32]. As seen in Fig. 15, spectra recorded 1.5, 4 and 200 μs after a flash show bleaching of the bands of XXI and appearance of two new sets of bands assigned to (η^4-1,3-C_4H_6)Fe(CO)$_2$(solv) and (η^4-1,3-*trans*-C_4H_6)Fe(CO)$_3$, XXII (shaded areas). At 4 μs, the bands assigned to the dicarbonyl species disappeared while those associated with the *trans*-butadiene isomer persist for almost 20 ms.

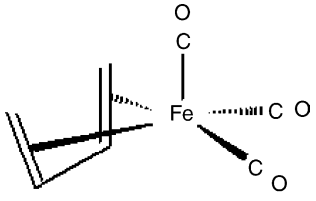

XXI

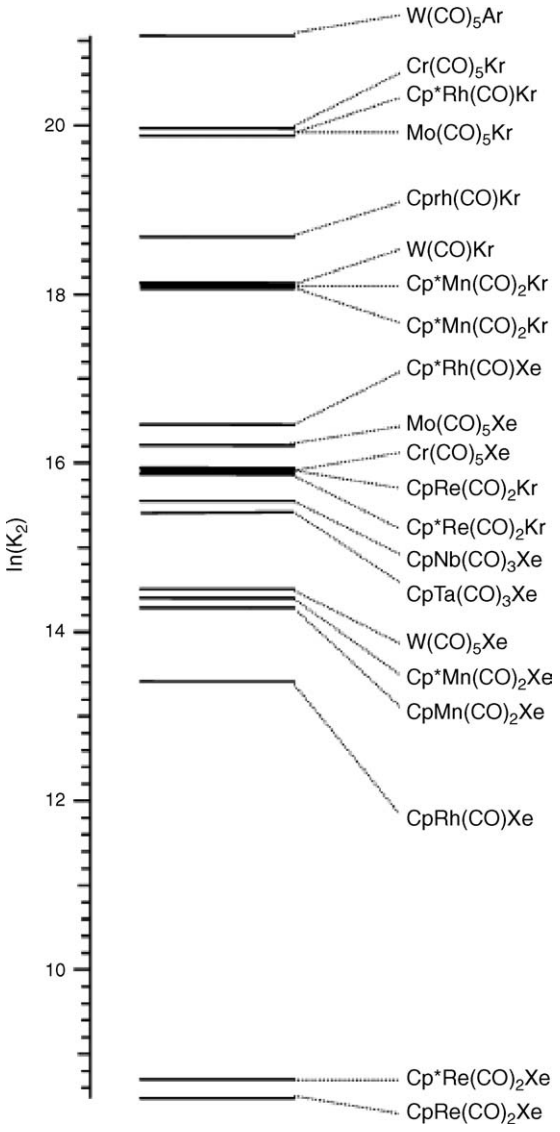

Fig. 14. Relative rates of reaction of noble gas complexes Cp′M(CO)$_n$L and M(CO)$_5$L with CO (Ref. [30]).

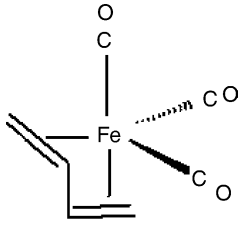

XXII

Photolysis of $Rh_4(CO)_{12}$ was monitored by time resolved step-scan IR and revealed the transformation of an initial transient species into a second species over the course of a 10 μs time window [33]. The spectra presented in Fig. 16 are averages of the first 10 spectra (i.e. first 200 ns of data) and the last 10 spectra at the end of the 10 μs window. Using the IR spectral patterns of structurally known analogues, the authors suggest the isomers shown to be likely candidates for the intermediates. The second transient species slowly recaptures CO.

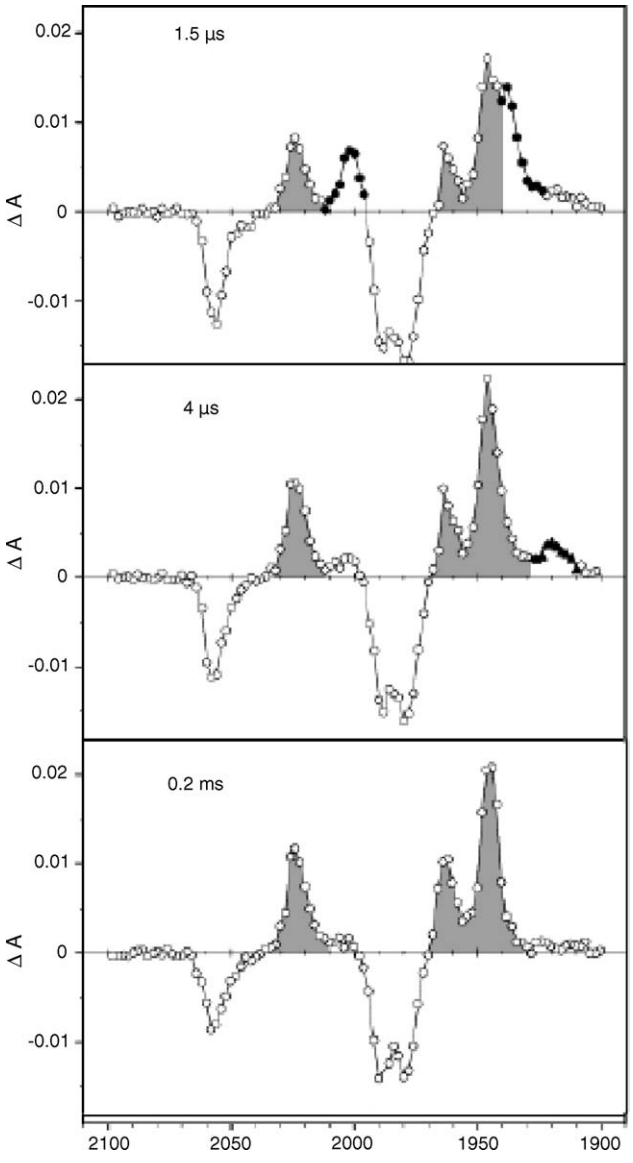

Fig. 15. Photolysis of (η^4-*cis*-1,3-C_4H_6)$Fe(CO)_3$. (η^4-*trans*-1,3-C_4H_6)$Fe(CO)_3$ (shaded area) (Ref. [32]).

Hamley et al. have described the photolysis of the Mn/Cr bimetallic compound, $(CO)_4Mn(\mu\text{-}\eta^3, \eta^6\text{-}C_3H_4\text{–}C_6H_5)Cr(CO)_3$, in frozen gas matrices [34]. In Ar photolysis resulted in exclusive loss of CO from Mn, while in N_2 both Mn and Cr CO-loss species were observed. Assignments were simplified in this case by the observation that the Mn and Cr portions of the molecule were vibrationally uncoupled, thus the use of model compounds $(CO)_4Mn(\eta^3\text{-}C_3H_4C_6H_5)$ and $(\eta^6\text{-}C_3H_4C_6H_5)Cr(CO)_3$ permitted assignment of bands in the bimetallic species.

Photolysis of cyclohexane solutions of $W(CO)_6$ and 2,5-dimethylfuran, $Me_2C_4H_2O$, has been found to result in initial formation of an oxygen bound furan, $W(CO)_5(Me_2C_4H_2O)$ which rapidly undergoes intramolecular rearrangement with loss of CO to yield $W(CO)_4(\eta^4\text{-}Me_2C_4H_2O)$, Scheme 10 [35]. This latter species could not be isolated, but it was characterized by IR and NMR spectroscopy.

Kunkley and Vogler have published several papers in which they examine the consequences of charge transfer transitions in metal complexes. For example, [36] they have examined the photochemical reaction of $[(\eta^5\text{-}C_6H_7)Fe(CO)_3]^+$ in aqueous solutions in order to examine the possible chemical consequences of a MLCT in which the formally cationic cyclohexadienyl ligand might assume anionic character in the excited state. Indeed it is found that MLCT excitations result in transfer of a proton from the solvent to the cyclohexadienyl ligand generating a cyclohexadiene ligand. Subsequent reaction of $[(\eta^4\text{-}C_6H_8)Fe(CO)_3]^{2+}$ with water results in ligand loss and decomposition of the complex. The authors describe this as a photochemical "umpolung" process since the cyclohexadienyl ring of the ground state is the point of attack by nucleophiles, while in the excited state it is susceptible to electrophilic attack.

A second paper by these workers have examined the photolysis of $[(\eta^3\text{-}C_3H_5)Pd(\mu\text{-}Cl)]_2$ [37]. It is known that this compound is light sensitive in acetonitrile solution. An analysis of the UV/visible spectrum in light of modern theoretical studies suggests that a band observed at 318 nm corresponds to a HOMO → LUMO transition. In this case, the HOMO and LUMO orbitals are composed of the ligand π_{nb} orbital and the metal d_{xy} orbital. The MO diagram of this molecule is presented in Fig. 17. The transition may be thought of as $(allyl)^{1-} \rightarrow Pd(II)$, the consequence of which is to oxidize the allyl anion to its corresponding radical, and generate Pd(I) which undergoes disproportionation in acetonitrile to give Pd(0) and $Pd(II)(CH_3CN)_2Cl_2$.

Bengali and Stumbaugh [38] have examined the flash photolysis of $Cr(CO)_6$ in a mixed benzene/heptane solvent in the presence of methylTHF ligands, Me_nTHF, where $n = 1$, 2 or 4.

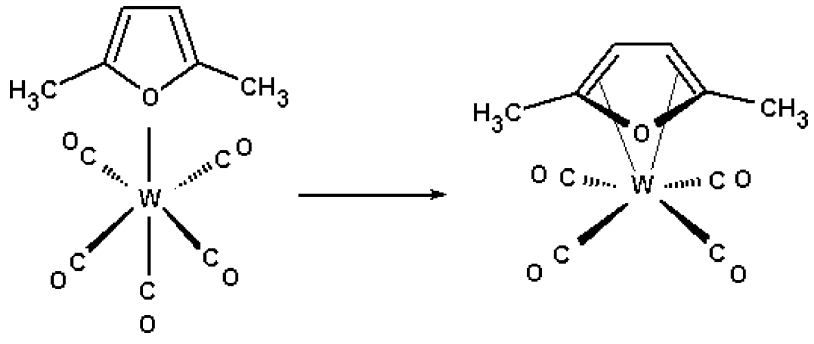

Scheme 10. (Ref. [35]).

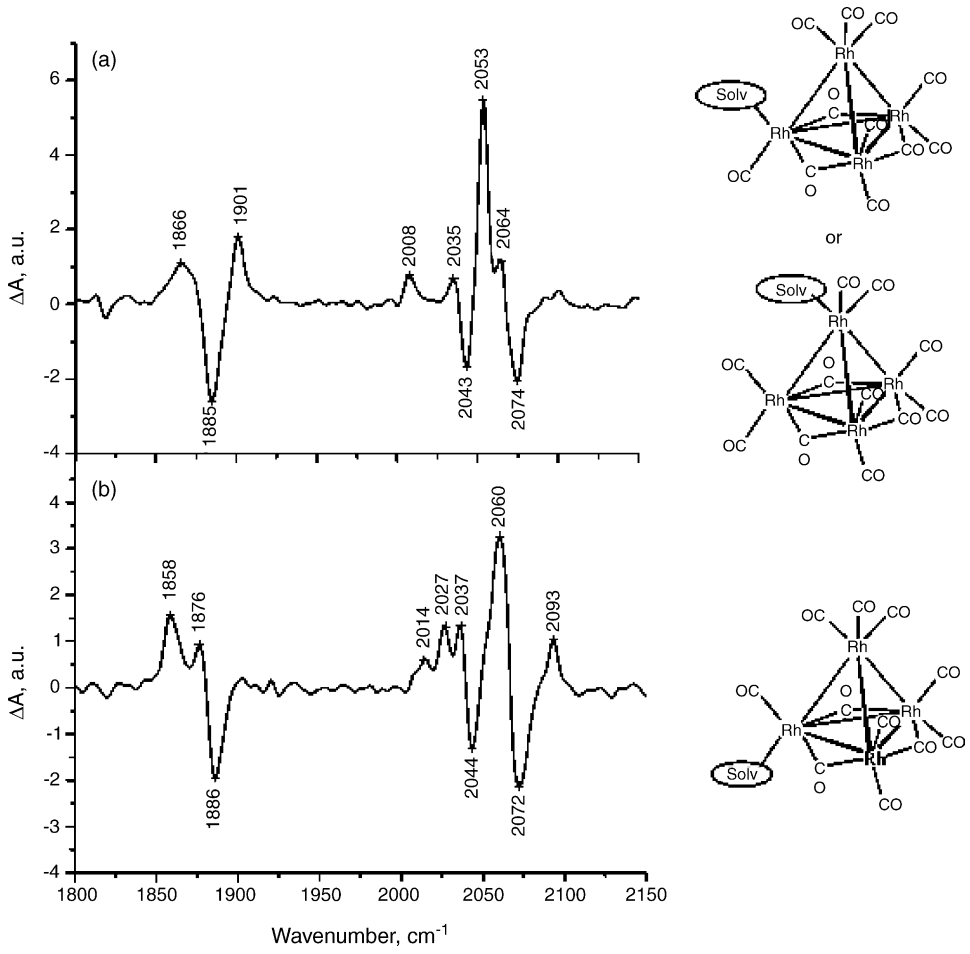

Fig. 16. Photolysis of $Rh_4(CO)_{12}$ in heptane. (a) Average of first 10 slices (200 ns) of the 10 μs time window. (b) Average of the last 10 slices of the time window (Ref. [33]).

In principle, photolysis of $Cr(CO)_6$ in the mixed solvent will lead to formation of both $Cr(CO)_5(\eta^2\text{-}C_6H_6)$ and $Cr(CO)_5$ (heptane), but the latter is known to be about 1000 times more reactive than the former. Therefore, steady state concentrations of the heptane species are expected to be quite low. The benzene complex and the product Me_nTHF complexes have distinct UV/vis absorption maxima, 520 and 420 nm, respectively, so they may be monitored simultaneously (Fig. 18). Analysis of the data suggests that two pathways are possible, Scheme 11, involving dissociative exchange, *D*, to yield the heptane complex, or interchange, I_d, leading directly to the Me_nTHF complex. The authors propose that the relative contributions of the two paths is dependent upon the ligand with MeTHF and Me_2THF proceeding through the I_d pathway while the more sterically bulky Me_4THF favors the dissociative pathway.

Closely related to the paper just discussed, Burkey and coworkers [39] have used laser induced optoacoustic spectroscopy to examine the enthalpies and volumes of reactions for the reaction of $Mo(CO)_6$ and tetrahydrothiophene, THT. In these experiments, an initial laser flash ejects CO from $Mo(CO)_6$ yielding $Mo(CO)_5$ (alkane) which then reacts with THT. Perhaps the most surprising observation was the determination of a bond energy of 155 ± 14 kJ/mol for Mo-THT, only slightly lower than that of Mo–CO, 170 ± 8 kJ/mol.

Lugovskoy et al. [40] have used step-scan time-resolved IR spectroscopy to examine the kinetics of photochemically generated $CpMn(CO)_2$ (solv) with cyclopentene, THF, furan and pyrrolidine to form $CpMn(CO)_2L$. Similarities in the positions of the carbonyl ligand stretching frequencies with those of known singlet species reported by Harris and co-workers [41] clarified the spin state of the solvated manganese species. Despite considerable ambiguity in the experimental results, the authors suggest that the reactions are best described as I_d mechanisms in which the transition state is early (the $\Delta H^{\ddagger}$ values are virtually independent upon the nature of the ligand).

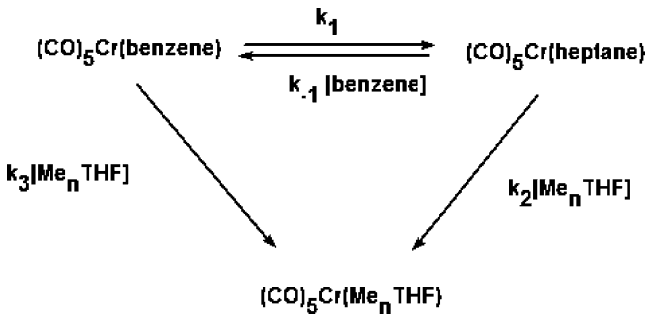

Scheme 11. (Ref. [38]).

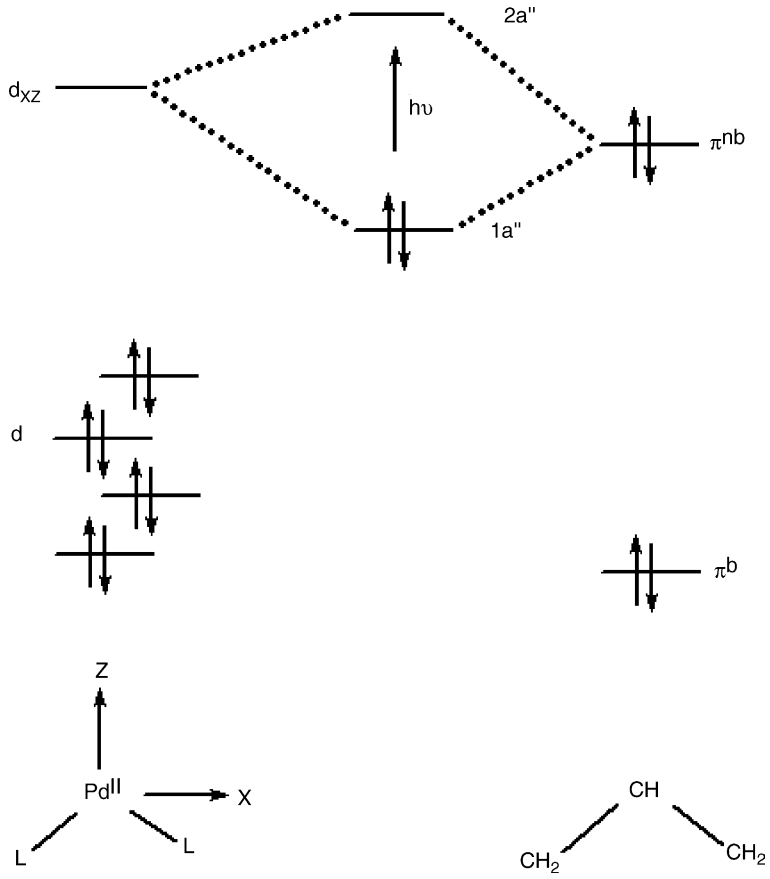

Fig. 17. Qualitative MO diagram for $(\eta^3\text{-}C_3H_5)PdL_2$ (Ref. [37]).

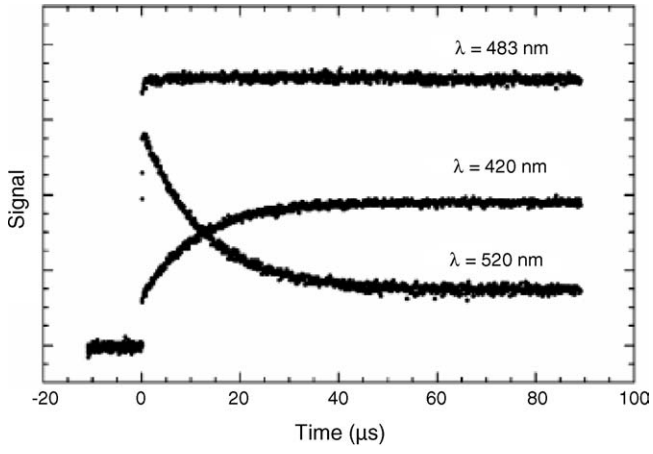

Fig. 18. Kinetic traces of the photolysis of a 3 mM solution of $Cr(CO)_6$ in benzene with 0.12 M THF at 293 K (Ref. [38]).

Andrews et al. have examined reactions of laser ablated group VI metals with CO in Ar and Ne matrices and find that a series of species $M(CO)_n$, where $n = 3$, 4, 5, are formed [42]. These species are analogous to the species observed in photochemical processes in frozen gas matrices.

Campos et al. have examined the photochemistry of group VI imine-carbene complexes with alkynes and have established the synthetic usefulness of this procedure for the production of 2-H-pyrrole derivatives [43]. The general reaction is illustrated in Scheme 12. Owing to experimental difficulties in examining the mechanism of the reaction, the authors employed dft techniques to calculate the energetics of the various presumed steps of the reaction. Unlike the analogous reaction between imine-carbene species and alkenes, there is no evidence either theoretical or experimental for a cyclopropene intermediate.

Schultz has reported a re-examination of the flash photolysis of Vaska's compound, $Ir(CO)(PPh_3)_2Cl$, in C_6D_6 [44]. Earlier studies by Wink and Ford used a broad band flash and UV/vis detection and provided data that was interpreted in terms of a

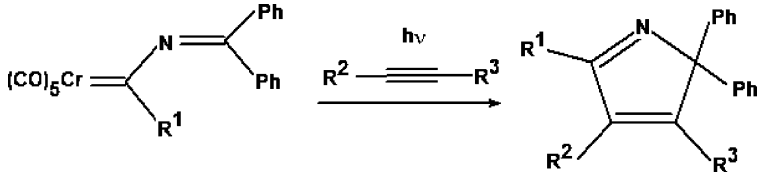

Scheme 12. (Ref. [43]).

three coordinate, CO-loss intermediate [45]. The rate of recovery of starting material was dependent upon CO concentration lending support to the three-coordinate intermediate hypothesis. The current studies were carried out using an XeCl excimer laser flash and the intermediates were followed by either step scan FTIR spectroscopy, or by a CW laser tuned to 1966 cm^{-1}, the carbonyl stretching frequency of the iridium compound. Curiously, upon photolysis the 1966 cm^{-1} band of the iridium compound decays exponentially over ca. 20 μs, while a new band, 1924 cm^{-1} grows in at the same rate. This peculiar behavior was interpreted in terms of the formation of a prompt intermediate, perhaps a long lived excited state triplet, having a carbonyl stretching frequency about the same as the starting material. This species is suggested to undergo dimerization and possible concurrent CO loss to yield the 1924 cm^{-1} species. The authors suggest that it is this dimer that was observed in the earlier investigation by Wink and Ford [46].

Over the last several years, Tyler and his co-workers have reported several studies of the radical cage effect, specifically related to the rates of radical recombination within the solvent cage versus diffusion from the solvent cage. These studies have been reviewed and offer an excellent summary of the earlier work [47]. This year the Tyler group has reported an examination of the effects of radical size, chain length and viscosity on radical recombination and diffusion for molybdenum bimetallic compounds of the general form, $[\eta^5\text{-}C_5H_4\text{–}CH_2CH_2N(CH_3)C(O)(CH_2)_nCH_3]_2Mo_2(CO)_6$, where $n = 3$, 8 or 18 [48]. A parameter termed the cage recombination efficiency is defined as $F_{cP} = k_{cP}/(k_{cP} + k_{dP})$, where k_{cP} is the radical recombination rate and k_{dP} is the diffusion rate. Previous studies involving silane substituents, $[\eta^5\text{-}C_5H_4\text{–}CH_2CH_2OSiR_3]_2Mo_2(CO)_6$, where R = Me, *i*-Pr, *n*-Pr or *n*-Hx, had established a relationship between k_{cP} and the mass of the radical and its radius, however, subsequent studies on molybdenum binuclear compounds in which there was a secondary amide in the pendant chain, $[\eta^5\text{-}C_5H_4\text{–}CH_2CH_2N(H)C(O)(CH_2)_nCH_3]_2Mo_2(CO)_6$, showed the k_{cP} to be independent of chain length. This puzzling finding was attributed to the possible formation of an agostic interaction between the amide N–H bond and the molybdenum atom. To further clarify the relationship between radical cage effect and chain length, the current study was initiated in which tertiary amide linkages, $[\eta^5\text{-}C_5H_4\text{–}CH_2CH_2N(CH_3)C(O)(CH_2)_nCH_3]_2Mo_2(CO)_6$, coupled the variable carbon chain to the molybdenum unit. As expected, the behavior of this latter compound was similar to that of the silane derivatives described above. An important innovation in the current work is the development of a modified equation to predict the ratio: k_{cP}/k_{dP}. According to Noyes [49], k_{cP}/k_{dP} should be linearly related to $m^{1/2}/r^2$, where m is the mass of the particle and r is the radius. In the current studies, the original assumption of spherical particles is invalid, so Tyler has substituted molecular surface and achieved good fits of the observed data.

Byun and Zink have examined the gas phase photolysis of CpCo(COD) as a model for the behavior of compounds used in laser assisted chemical vapor deposition [50]. The authors describe three surprising features of this photolysis in that significant quantities of the intact molecular ion were observed, both $CpCo^+$ and $Co(COD)^+$ were observed with a strong wavelength dependence upon the relative proportions of the two species, and fragmentation of the original ligands occurred leaving portions of these ligands bound to the metal. The relative ratios of $CpCO^+$ to $Cp(COD)^+$ are attributed to the nature of the excited states being populated at the different wavelengths. This is nicely illustrated by Fig. 19. The observation of intact molecular fragments at the highest energy photolysis, 266 nm, is particularly surprising. The vertical ionization energy of CpCo(COD) has been reported to be 6.96 eV [51], corresponding to 1.5 photons of 266 nm. The average cyclopentadienyl bond disruption enthalpy for cobaltocene has been measure to be 1.58 eV [52], therefore the 266 nm photon carried more than sufficient energy for removal of ligands, but less than that necessary for ionization.

Hall and co-workers [53] have carried out photochemical studies and supporting theoretical calculations to develop an understanding of the factors necessary to achieve C–H activation at metal centers. Some time ago, Hartwig established that catachol borane derivatives of the type $Cp^*M(CO)_nBcat$, where M = Fe, $n = 2$ or M = W, $n = 3$, XIX, undergo photolysis in the presence of hydrocarbons to yield R-Bcat derivatives [54]. In the current study, photolysis of $CpFe(CO)_2(\eta^1\text{-}p\text{-toluyl})$ or $Cp^*W(CO)_3(\eta^1\text{-}p\text{-toluyl})$ in benzene yielded no evidence for oxidative addition of Ph-H and loss of toluene, although ^{13}CO exchange and PMe_3 substitution established that CO-loss was taking place. $Cp^*Fe(CO)_2$(borazinyl) in which the boron p orbital is involved in π bonding was prepared and photolyzed in benzene with no evidence of formation of borazinyl-Ph derivatives. In order to understand the role of an empty boron p-orbital, dft calculations were carried out which suggested the reaction sequence presented in Scheme 13 as a plausible mechanism. In this sequence hydride transfer is accomplished through two σ-bond metathesis steps.

Finally, in this section we note a recent paper from the Vrije Universiteit theoretical group [55]. These workers have made major contributions to the understanding of the excited states of transition metal carbonyl compounds and have overthrown the existing paradigm, which viewed the lowest excitation states as ligand field transitions. TDDFT studies clearly establish that the set of carbonyl π^* orbitals lie below the virtual metal d orbitals, thus the lowest excitations are MLCT bands and not LF bands. These theoretical approaches have been applied to the analysis of PH_3 complexes of Cr and Fe. It is found that the excited states of $Cr(CO)_5PH_3$ are repulsive for PH_3 but modestly bonding for CO, i.e. there is a small energy barrier at a M–CO distance beyond the equilibrium distance. In contrast, the lowest excited state for $Fe(CO)_4PH_3$ is a LF state which is repulsive for both PH_3 and CO although loss of PH_3 is strongly preferred.

3. Photocatalysis

Akioka et al. have examined the photo-assisted hydrogen transfer hydrogenation of norbornadiene and its valence isomer quadricyclane using $Rh_6(CO)_{16}$ as a catalyst precursor [56]. Norbornadiene and quadricyclane are photochemically inter-

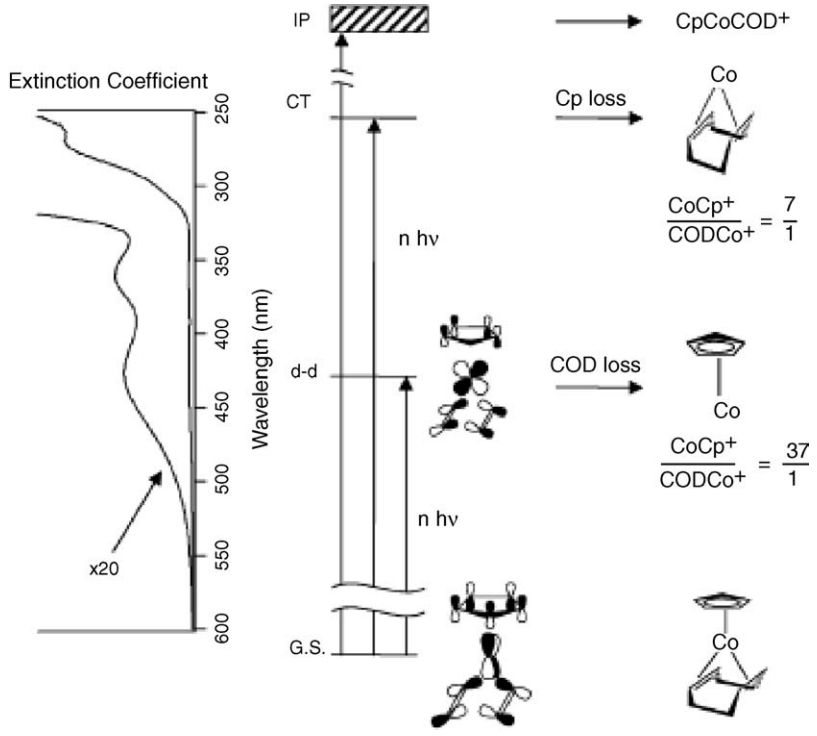

Fig. 19. Schematic energy level diagram illustrating the states initially populated and the resulting fragmentation reactions (Ref. [50]).

changeable in the presence of acetone, thus some rearrangement of the two species occurs under the conditions of the catalytic studies. As a result, analysis of the species in solution during the reactions, Fig. 20a, reveals the presence of quadricyclane in both systems. A proposed reaction scheme is presented in Fig. 20b. Consistent results were only achieved when the rhodium catalyst was "formed" by photolysis prior to addition of the carbocyclic reactants. The exact composition of the catalyst is not clear.

Wang and Necker have examined the photochemical isomerization of linear olefins by $Pt(acac)_2$ and silanes and found that

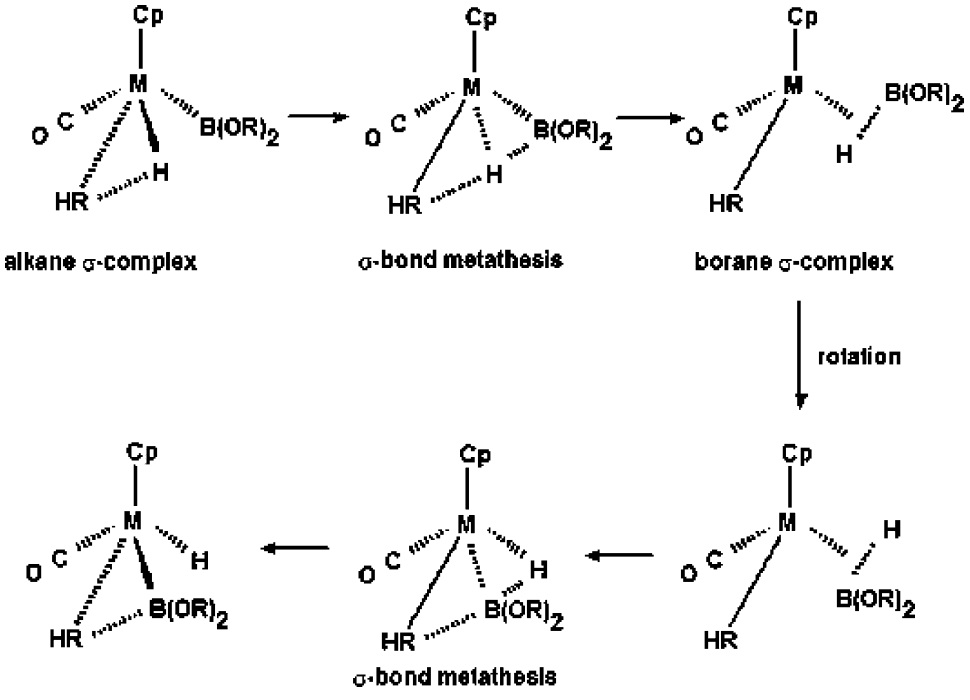

Scheme 13. Proposed mechanism of ligand rearrangement in reactions of alkanes with metal borazinyl compounds (Ref. [53]).

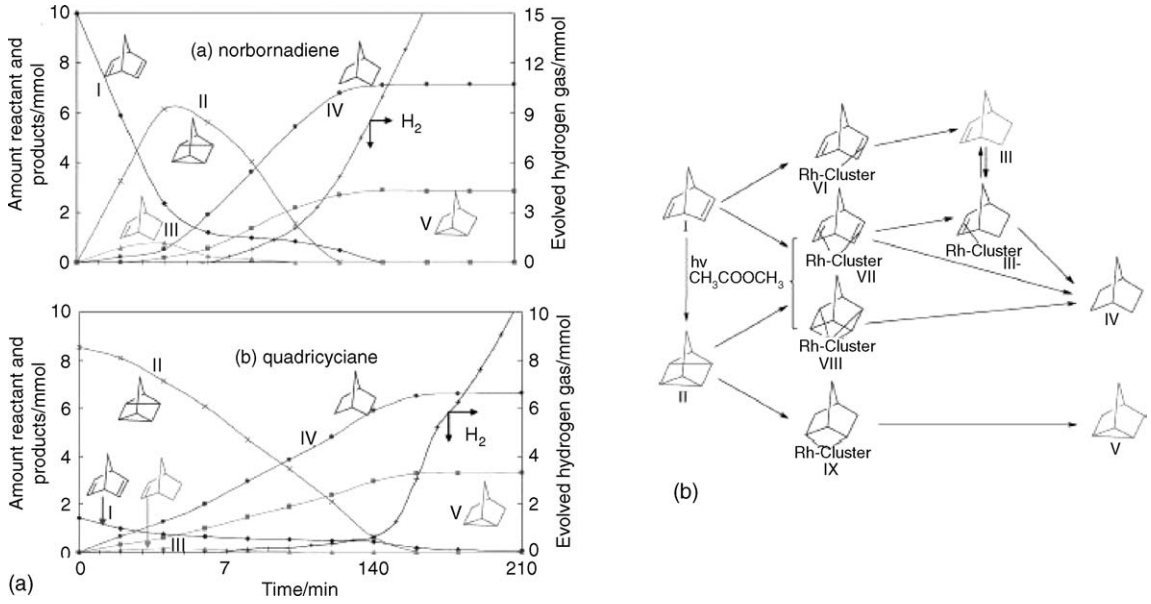

Fig. 20. (a) Compositional analysis of reaction mixtures. (b) Proposed reaction mechanism (Ref. [56]).

the efficiency of the process is dependent upon the nature of the silane with Ph_3SiH giving the best yields [57]. The proposed mechanism of this reaction (Scheme 14), presumes the coordination of both the silane and olefin on the Pt with the rearrangement mediated by proton transfer to and from the silane. This very interesting proposal raises the question of whether the hydrogen is transferred by σ-bond metathesis or oxidative addition of the Si–H to the Pt followed by transfer to the olefin.

Badarau and Wang have examined the $W(CO)_6$ photocatalyzed cross linking of polymers containing acetylene units [58]. The polymers were prepared by free radical polymerization of propragyl acrylate and methyl methacrylate. IR examination of the reaction mixtures during the photolysis established the presence of $W(CO)_5$ (acetylene) groups and it is presumed that subsequent CO-loss to the tetracarbonyl generates the active species.

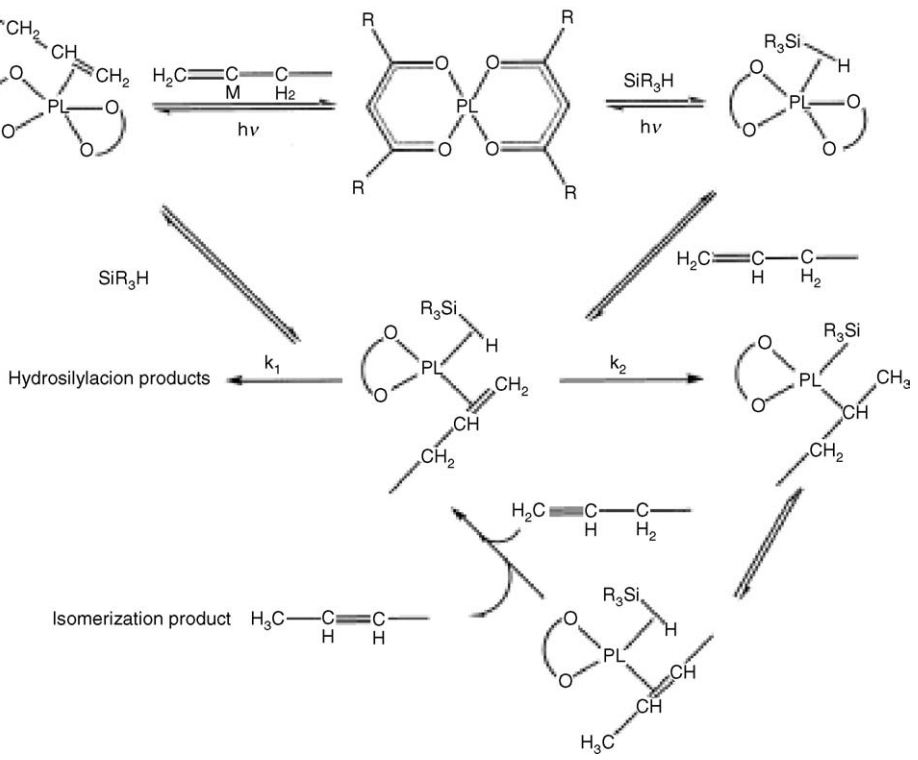

Scheme 14. This scheme has been corrected from that originally reported with the kind permission of the author (Ref. [57]).

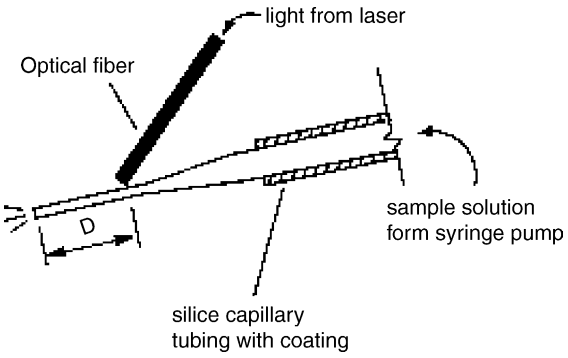

Fig. 21. Schematic drawing of the position of the optical fiber relative to the end of the electrospray tip (Ref. [61]).

Kutal has published a useful review of iron metallocenes that may be used in the photoinitiation of ionic polymerization reactions [59]. Apropos to this Wang and Huang [60] have described the use of CpFe(naphthalene) cations as sensitive photoinitiators for epoxide polymerization. In the case of conventional ferrocene, CpFe(arene) and these CpFe (naphthalene) precursors the actual catalytic species is presumed to be $[CpFe]^+$.

Kutal and co-workers [61] have exploited electrospray MS as a tool in the analysis of the mechanism of photoinitiated polymerization. By placing a fiber-optic light source near the output of the quartz electrospray tip, the time between photolysis and vaporization into the MS chamber could be directly controlled, Fig. 21. Two significant experiments were performed. In one, the intermediacy of $[CpFe(MeCN)_3]^+$ in the photolysis of $[CpFe(arene)]^+$ in acetonitrile was established, while in the second photolysis of $[CpFe(arene)]^+$ in dichloroethane solutions containing cyclohexene oxide (CHO) resulted in formation of species of the form $[CpFe(H_2O)(CHO)_{0–5}]^+$, and ring de-ligated species of the form $[Fe(H_2O)(CHO)_{2–12}]^{+2}$. These latter species appear to have captured the growing polymer chain in its earliest moments.

4. Diimine photochemistry and photophysics

Diimine complexes have been studied extensively as model compounds for which charge transfer processes dominate the photochemistry. Recently techniques, such as time resolved IR and time-resolved resonance Raman have been employed to explore the excited states of these species in some detail. For example, we have already presented time-resolved IR spectra of *fac*-$[Re(CO)_3(dppz)py]^+$ and *fac*-$Re(CO)_3(dppz)Cl$ (Fig. 13). These compounds, XXIII, have also been examined by time-resolved resonance Raman and from these complementary data a proposed Jablonsky diagram was developed, Fig. 22 [62]. In this diagram near UV excitation promotes an electron to either ^{1}MLCT or ^{1}IL Frank–Condon excited states, with the latter likely arising from a $d\pi(Re) \rightarrow \pi^*$ (phen) transition. These states might relax to their corresponding triplet states followed by a series of intersystem conversions leading to an emissive state that is likely to be the ^{3}IL(phz). This latter state is believed to be in equilibrium with a close lying ^{3}MLCT state.

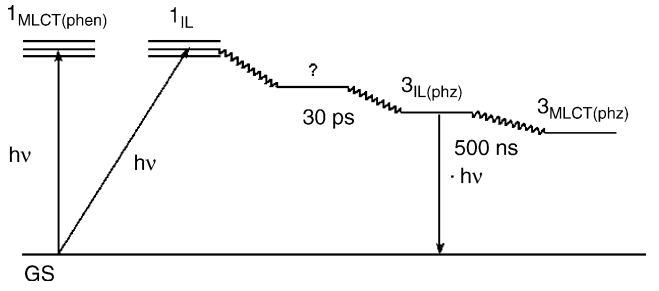

Fig. 22. Proposed Jablonsky diagram for *fac*-$[Re(CO)_3(dppz)py]^+$ (Ref. [62]).

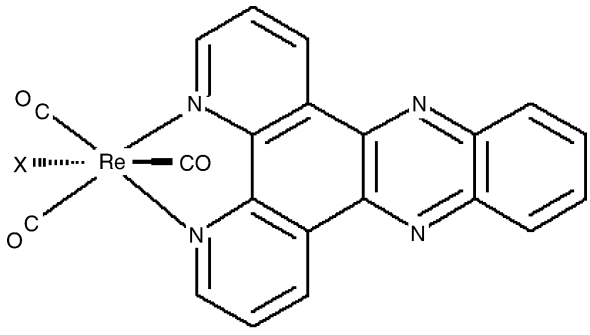

X = py or Cl

XXIII

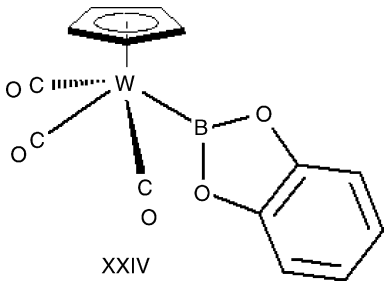

XXIV

Dattelbaum et al. have examined the photochemical transformation of the 1,2-bis(4-pyridyl)ethene, bpe, ligand in *fac*-$[Re(CO)_3(phen)bpe]^+$ from trans to cis upon excitation at 355 nm, Scheme 15 [63]. Time-resolved IR measurements (Fig. 23), demonstrate that the carbonyl bands of the excited state species are shifted slightly down in energy. Since MLCT transitions result in instantaneous oxidation of the metal center those transitions are typically accompanied by large shifts of carbonyl stretching frequencies to higher energy. The small downward shift in the current case suggested that the transient observed here has an excited state located on the *trans*-bpe ligand. The short lifetime of this state ($\tau = 28$ ns) suggested a ^{3}p as the immediate precursor to the trans → cis conversion. The proposed sequence of events in the photochemistry of this compound is suggested to be initial formation of the Frank–Condon ^{1}MLCT or $\pi\pi^*$ states that decay to a ^{3}MLCT and further to $^3t^*$ and $^3p^*$, where $^3t^*$ is the excited state of the trans double bond.

Iha and co-workers have examined the closely related *fac*-$[Re(phen)(CO)_3(cis\text{-}bpe)]^+$ and its bimetallic analogue and have demonstrated that the emission behavior is strongly influenced by solvent rigidity [64]. Absorption bands are only slightly affected by solvent rigidity as expected for a Frank–Condon

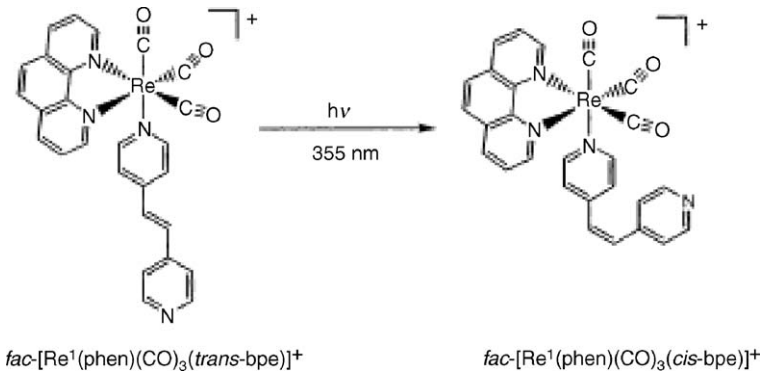

Scheme 15. *Trans* to *cis* conversion of the 1,2-bis(4-pyridyl)ethene ligand (Ref. [63]).

excitation to a ^{1}MLCT state, while the emission bands experience a substantial hypsochromic shift related to the rigidity of the medium. The authors suggest that the relative energy of the ^{3}MLCT state increases with increasing rigidity of the medium so that in highly rigid environments, such as frozen glasses at 77 K the ^{3}MLCT actually lies above the ^{3}IL. One consequence of this crossover is apparent in comparing the emission lifetimes, which are on the order of 100 ns in EPA (diethyl ether/isopentane/ethanol) at room temperature but on the order of microseconds at 77 K.

Fujita and co-workers [65] have examined the photochemistry of $[Re(dmb)(CO)_3(CH_3CN)]PF_6$ and $Re(dmb)(CO)_3Cl$, where dmb = 4,4′-dimethyl-2,2′-bipyridine, and their one electron reduction products. Flash photolysis of these compounds coupled with time-resolved IR results in formation of an excited state triplet which has carbonyl stretching frequencies shifted to higher energy characteristic of an MLCT transition (Fig. 24a). Photolysis in the presence of a reducing agent, such as triethylamine, TEA, results in the formation of the one electron reduction products, $Re(dmb)(CO)_3(CH_3CN)$ or $[Re(dmb)(CO)_3Cl]^{-1}$. The spectra of these species have been directly observed (Fig. 24b). The extra electron is believed to reside in the dmb π^* orbital. Partial occupancy of this orbital reduces the back-bonding between the dmb and the Re. Rhenium electron density is thus redirected into the carbonyl backbond resulting in a decrease in the stretching frequencies of these ligands as seen in the time-resolved IR. Reduction of $Re(dmb)(CO)_3(OTf)$ in THF by sodium amalgam results in formation of the Re–Re bonded dimer, $[Re(dmb)(CO)_3]_2$. Photolysis of this species results in the formation of $Re(dmb)(CO)_3$

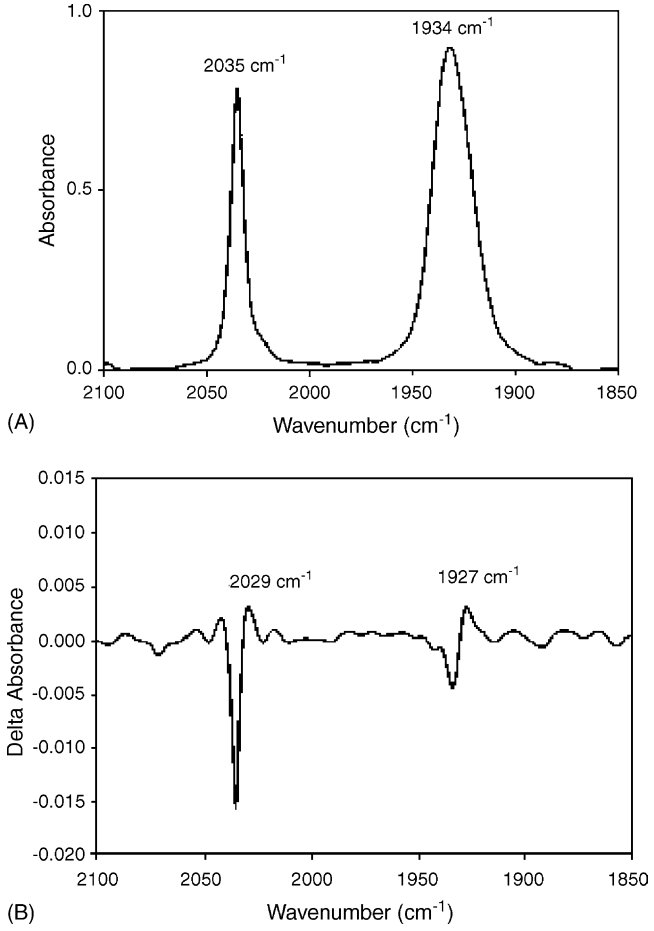

Fig. 23. Ground state (A) and (B) TRIR spectrum of *fac*-$[Re(CO)_3(phen)(bpe)]^+$ in CH_3CN. TRIR spectrum is recorded from cessation of 355 nm flash to 50 ns (Ref. [63]).

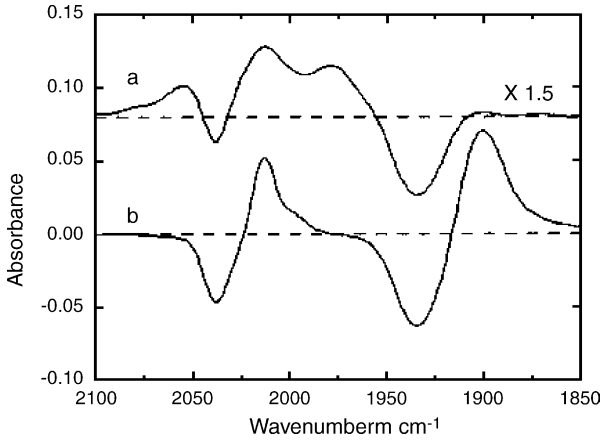

Fig. 24. Transient FTIR (difference) spectra of a CH_3CN solution containing $[Re(dmb)(CO)_3(CH_3CN)]PF_6$: (a) excited state spectrum under Ar and (b) photoformed singly reduced species with TEA under Ar (Ref. [65]).

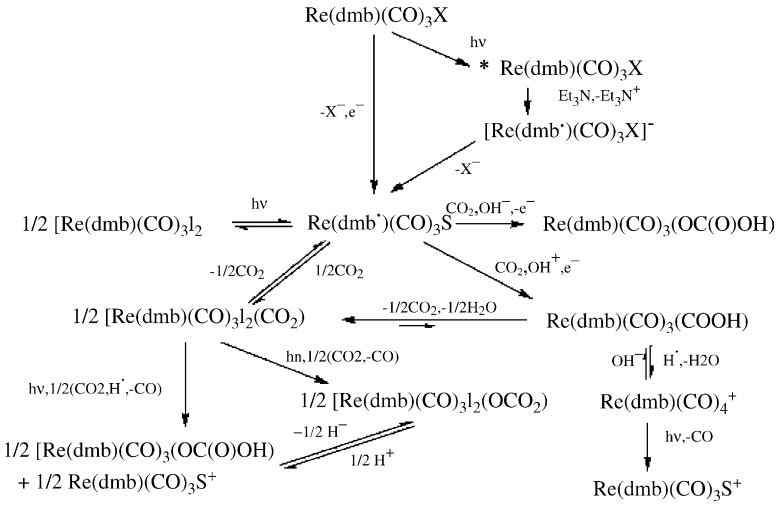

Scheme 16. Reactions of Re(dmb)(CO)$_3$S with CO_2 (Ref. [65]).

which reacts with solvent to yield Re(dmb)(CO)$_3$S in which, as in the one electron reduced species above, the extra electron is in the dmb π^* orbital. Reformation of the dimer is slow due to the pre-equilibrium rearrangement requiring loss of solvent before the metal based radical can reform. In the presence of CO_2, Re(dmb)(CO)$_3$S yields several products as illustrated in Scheme 16.

In a closely related result Hori et al. described the photoreduction of CO_2 to CO under high pressure CO_2 [66]. Triethylamine is used as the sacrificial electron donor for the process. A proposed catalytic cycle is presented in Scheme 17. It is proposed that the higher pressure of CO_2 prevents formate formation by rapidly trapping the electron deficient intermediate, compound 3 in Scheme 17, before protonation can set up conditions for formate production.

Yam et al. have examined the luminescent behavior of Re(bipy)(CO)$_3$(C$_2$R), where R represents a range of organic groups [67]. The molecular structure of Re(bipy)(CO)$_3$(C$_2$Ph) is presented in Fig. 25. The compounds all display an intense orange emission from what is believed to be a triplet ligand centered excited state. Molecular orbital analysis of the molecule reveals that the initial excitation may be a combination of a dπ(Re) $\rightarrow \pi^*$(bipy) transition and a (CC) $\rightarrow \pi^*$(bipy) LLCT.

Záliš et al. have added to a growing body of experimental and theoretical work that is overturning long held preconceptions concerning the role of ligand field, LF, transitions in metal complexes [68]. This paper examines the photophysics of W(CO)$_4$(DAB) and W(CO)$_4$(en) and in particular provides time-resolved IR and resonance Raman support for the proposal that MLCT bands are responsible for the observed spectral features. The electronic spectra of W(CO)$_4$(en) and W(CO)$_4$(*i*-Pr-DAB) are presented in Fig. 26. Nor surprisingly, sophisticated DFT calculations assign the intense low energy, 2.33 ev (531 nm), band of W(CO)$_4$(*i*-Pr-DAB) to a W $\rightarrow$ DAB MLCT. The bands at 3.30 ev (376 nm) in the spectrum of W(CO)$_4$(*i*-Pr-DAB) and those at 2.71 ev (458 nm) and 3.12 ev (458 nm) in the spectrum of W(CO)$_4$(en) are assigned to W(CO$_{eq}$) $\rightarrow$ (CO$_{ax}$)

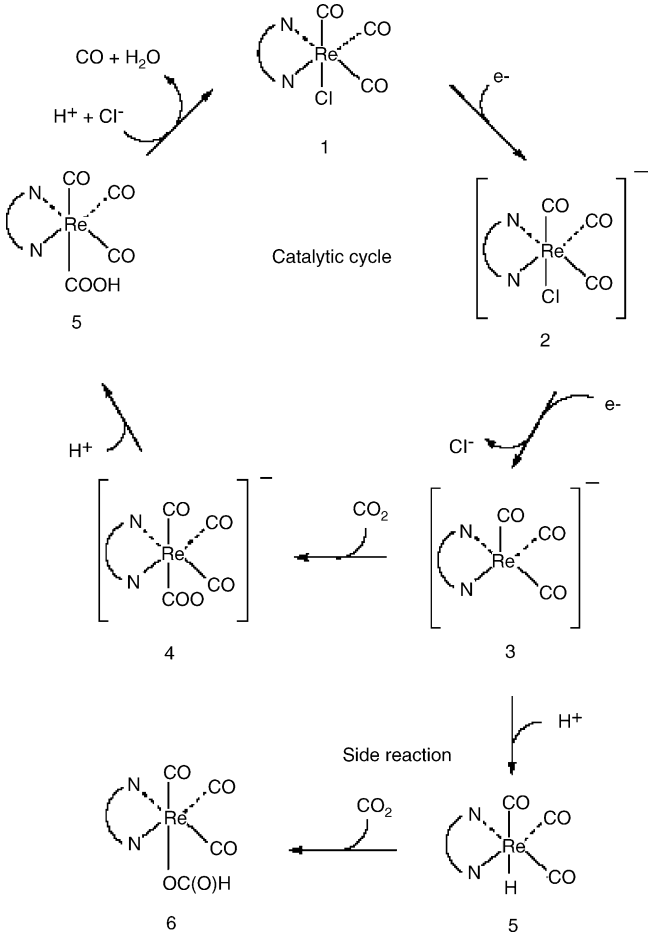

Scheme 17. Catalytic cycle for the photochemical reduction of CO_2 to CO (Ref. [66]).

transitions. In the latter case, the weak band at 2.71 ev is assigned to a spin-forbidden $a^1A \rightarrow a^3A$ transition. For W(CO)$_4$(en), both time-resolved IR and resonance Raman demonstrate that the carbonyl ligands are involved in the two low lying transitions. What

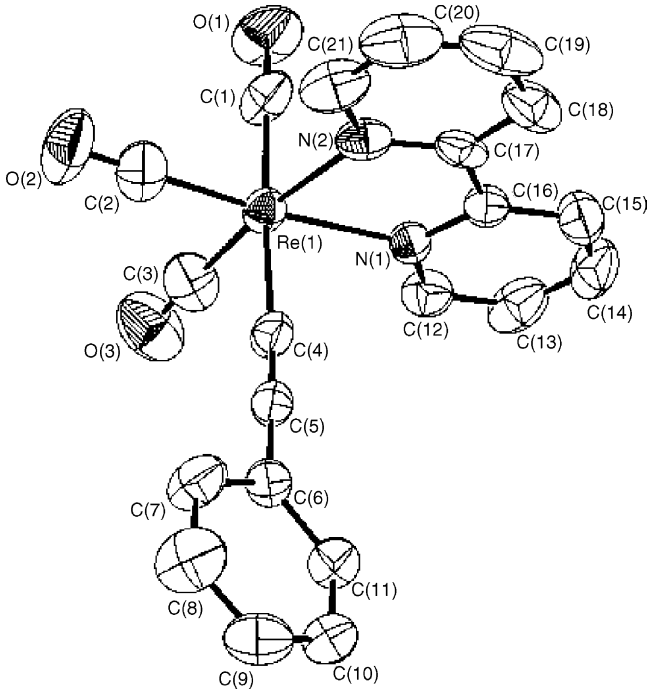

Fig. 25. Molecular structure of Re(bipy)$(CO)_3(C_2Ph)$ (Ref. [67]).

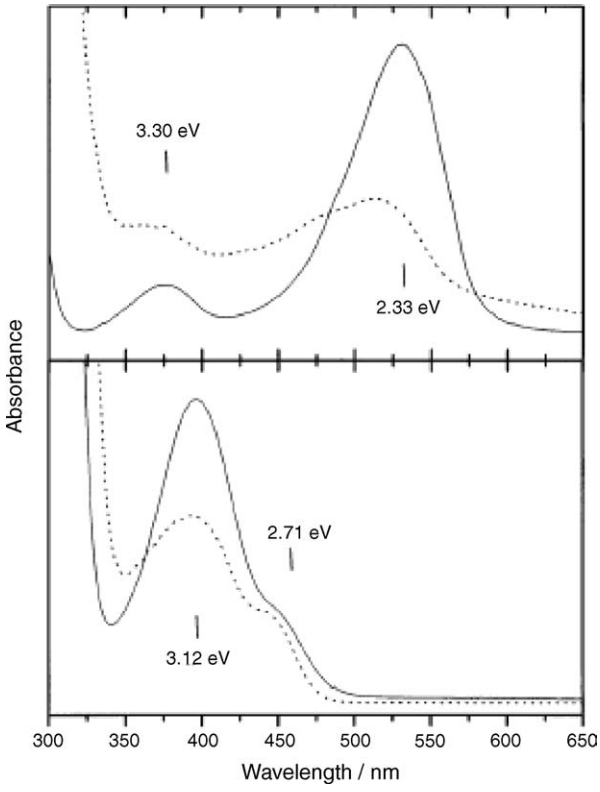

Fig. 26. Electronic spectra of $W(CO)_4$(*i*-Pr-DAB) (top) and $W(CO)_4$(en) (bottom), in CH_2Cl_2 and CH_3CN, respectively. Dashed lines are diffuse reflectance spectra (Ref. [68]).

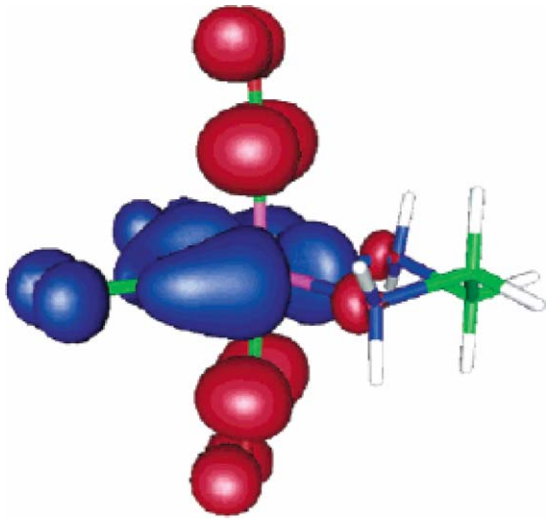

Fig. 27. Change in electron density distribution upon the $a^1A \rightarrow a^1B$ electronic transition. Blue and red colors correspond to a decrease and increase in electron density, respectively (Ref. [68]).

is perhaps most significant in the analysis of the electronic spectra of these compounds is the absence of LF transitions at any reasonable energy. Going from DAB to en removes the relatively low energy DAB π^* orbitals leaving the CO π^* orbitals as the next accessible level. The donor and acceptor orbitals are beautifully illustrated in Fig. 27.

Vergeer et al. have examined the photochemistry of the ruthenium cluster compounds, $Ru_3(CO)_8(\eta\text{-}CO)_2(\alpha\text{-diimine})$, where diimine = 2,2′-bipyridine,4,4′-dimethyl-2,2′-bipyridine and 2,2′-bipyrimidine [69]. Resonance Raman spectroscopy demonstrates that the lowest allowed electronic transition at 471 nm is strongly coupled with α-diimine internal stretching modes, as well as with the symmetric carbonyl stretching modes and M–C–O deformation modes. The authors suggest that the cluster core as well as the α-diimine ligand participate in the electronic changes associated with this excitation. Time resolved IR studies on the ps time scale reveal that the bridging carbonyl ligand stretching frequency increases by 35 cm^{-1}, while the terminal carbonyl stretching frequencies decrease. This feature is consistent with DFT calculations that assign the HOMO orbital to the $Ru_2(\mu\text{-}CO)_2$ grouping, while the LUMO is heavily α-diimine centered.

5. Metal nitrosyl photochemistry

Mascharak and co-workers have prepared iron nitrosyl derivatives of the pentadentate ligand, *N*,*N*-bis(2-pyridylmethyl) amine-*N*-ethyl-2-pyridine-2-carboxamide [$PaPy_3$] in both the Fe(II) and Fe(III) oxidation states [70]. The molecular structure of $Fe(PaPy_3)NO]^{2+}$ is presented in Fig. 28. Photolysis of the Fe(III) species in several solvents with a tungsten lamp initiated the loss of NO. In CH_3CN a solvate complex, $[Fe(PaPy_3)(CH_3CN)]^{2+}$ was isolated and it was shown that excess NO reacted with this species to reform the nitrosyl compound. This appears to be the first example of reversible nitrosyl

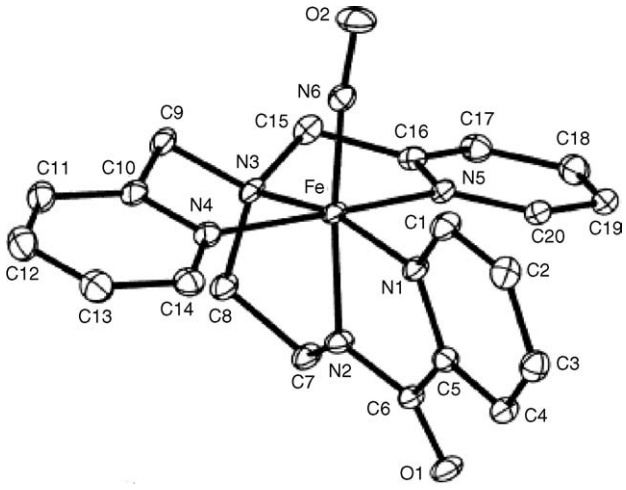

Fig. 28. Molecular structure of $[Fe(PaPy_3)(NO)]^{2+}$ (Ref. [70]).

binding in a non-heme Fe(III) complex. Curiously, the Fe(II) species does not exhibit NO loss upon photolysis.

Ford and co-workers have examined the photolysis of Roussin's red salt esters, $Fe_2(NO)_4(\mu\text{-}SR)_2$, where R = Me, Et, Bz, $(CH_2)_2OH$ and $(CH_2)_2SO_3^{-1}$ [71]. Continuous photolysis was monitored by an NO electrode and demonstrated that four NO molecules are released for every Roussin's red salt ester. Flash photolysis (355 nm) studies under NO or Ar demonstrated that NO loss is reversible, Fig. 29a, exhibiting second order kinetics in [NO] and the NO-loss species. In contrast, photolysis under O_2, Fig. 29b, indicates a competition between NO and O_2 for the intermediate. It is argued that the third-order reaction of NO with O_2 is too slow to significantly affect the kinetics.

Andrew et al. [72] have examined the photolysis of a cytochrome *c′* protein of *alcaligenes xylosoxidans*, 5c-NO AXCP, known to have an NO bound to the heme in the proximal position [73]. Flash photolysis (532 nm), Fig. 30, resulted in bleaching of the Soret band of 5c-NO AXCP and appearance of bands attributable to the NO-free, 5c-Fe(II) and distal NO bound, 6c-NO species. In an excess of NO the proximal 5c-NO species reforms over time. The blocking of the proximal face by rebinding of the histidine group serves as a kinetic trap that precludes simple reattachment of NO to this face. Proximal binding is facilitated by NO binding to the distal face of the heme,

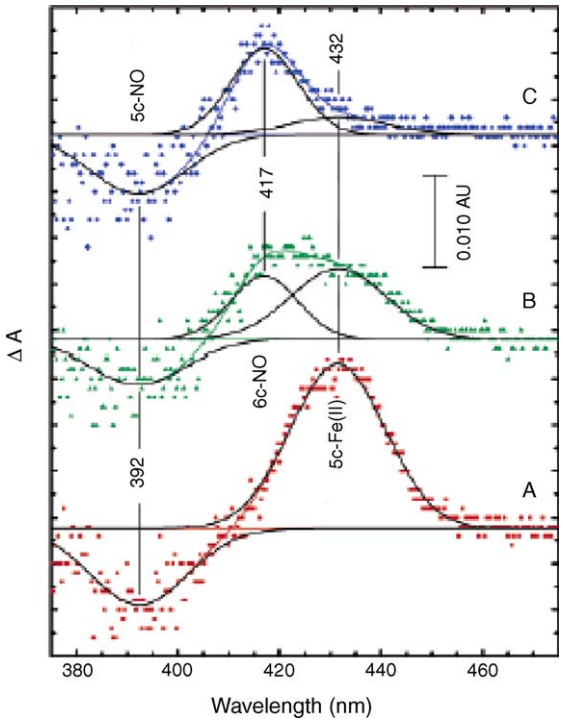

Fig. 30. Transient Δ*A* spectra of the photolysis of 5c-NO AXCP (A) 5, (B) 15 and (C) 50 ms after a 3 ns pulse of 532 nm light (Ref. [72]).

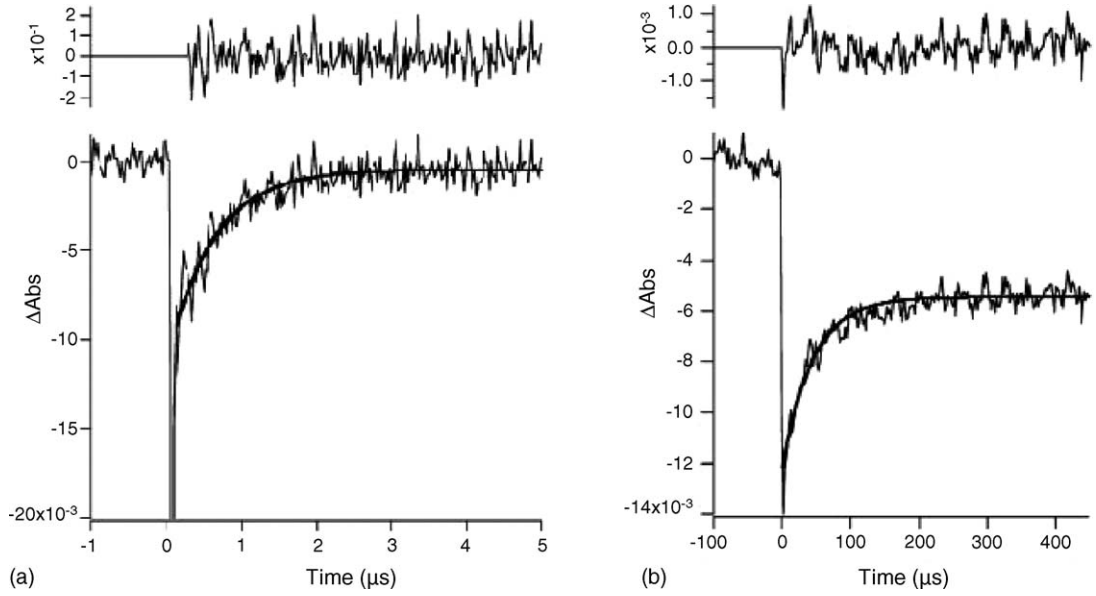

Fig. 29. (a) Flash photolysis of Na_2 $[Fe_2(NO)_4(\mu\text{-}S(CH_2)_2SO_3)_2]$ (36.3 μM) in water solution under NO (1.07 mM) as monitored at 420 nm. (b) Flash photolysis of $Fe_2(NO)_4(\mu\text{-}S(CH_2)_2OH)_2$ (36.3 μM) in aerated methanol ($[O_2]$ = 1.8 mM, T = 294 K) as monitored at 420 nm (Ref. [71]).

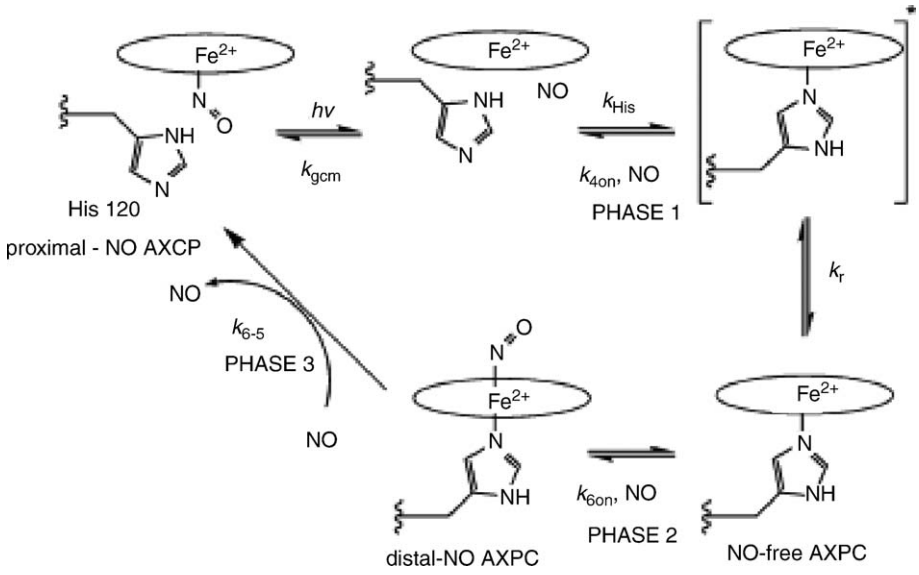

Scheme 18. Proposed mechanism of NO binding and photochemical release from 5c-NO AXCP (Ref. [72]).

thus weakening the his-Fe interaction and allowing insertion of NO. The proposed mechanism of this process is illustrated in Scheme 18.

References

[1] T.E. Bitterwolf, Photochemistry of transition metal complexes, in: R.B. King (Ed.), Encyclopaedia of Inorganic Chemistry, second ed., J. Wiley and Sons, 2005.
[2] T.E. Bitterwolf, J. Organomet. Chem. 689 (2004) 3939.
[3] D.J. Darensbourg, M.J. Adams, J.C. Yarbrough, A.L. Phelps, Eur. J. Inorg. Chem. (2003) 3639.
[4] U. Oezdemir, N. Karacan, O.S. Şentürk, S. Sert, F. Ugur, Trans. Met. Chem. 28 (2003) 443.
[5] O.S. Şentürk, U. Oezdemir, S. Sert, N. Karacan, F. Ugur, Inorg. Chem. Commun. 6 (2003) 926.
[6] S. Sert, A. Ercag, O.S. Şentürk, B.T. Sterenberg, K.A. Vdachin, Ü. Özdemir, F.U. Sarikahya, Polyhedron 22 (2003) 1689.
[7] O.S. Şentürk, H.A. Shekhel, B.T. Sterenberg, K.A. Vdachin, S. Sert, Ü. Özdemir, F.U. Sarikahya, Polyhedron 22 (2003) 1659.
[8] P. Mathur, A.K. Bhunia, C. Srinivasu, S.M. Mobin, J. Organomet. Chem. 670 (2003) 144.
[9] (a) P. Mathur, M.O. Ahmed, J.H. Kaldis, M.J. McGlinchey, J. Chem. Soc., Dalton Trans. (2002) 619;
(b) P. Mathur, M.O. Ahmed, A.K. Dash, M.G. Walawalkar, V.G. Purank, J. Chem. Soc., Dalton Trans. (2000) 2916.
[10] F. Godoy, A.H. Klahn, F.J. Lahoz, A.I. Balana, B. Oelckers, L.A. Oro, Organometallics 22 (2003) 4861.
[11] J. Müller, C. Hirsch, K. Ha, Z. Anorg. Allg. Chem. 629 (2003) 2180.
[12] Y. Zhang, K.H. Pannell, Organometallics 22 (2003) 1766.
[13] K.H. Pannell, T. Kobayashi, F. Cervantes-Lee, J. Organomet. Chem. 685 (2003) 189.
[14] Y. Zhang, F. Cervantes-Lee, K.H. Pannell, Organometallics 22 (2003) 2517.
[15] H. Okada, M. Okazaki, H. Tobita, H. Ogino, Chem. Lett. 23 (2003) 876.
[16] M. Okazaki, M. Iwata, H. Tobita, H. Ogino, J. Chem. Soc., Dalton Trans. (2003) 1114.
[17] D.G. Churchill, J.H. Shin, G. Parkin, J. Chem. Cryst. 33 (2003) 297.
[18] D.M. Thompson, M. Jones, M.C. Baird, Eur. J. Inorg. Chem. (2003) 175.
[19] K. Matsubara, S. Niibayashi, H. Nagashima, Organometallics 22 (2003) 1376.
[20] T. Miura, K. Kiyota, H. Kusama, K. Lee, H. Kim, S. Kim, P.H. Lee, N. Iwasawa, Chem. Lett. 5 (2003) 1725.
[21] P. Wipf, T.H. Graham, J. Org. Chem. 68 (2003) 8798.
[22] A. Aballay, F. Godoy, G.E. Buono-Core, A.H. Klahn, B. Oelckers, M.T. Garland, J.C. Munoz, J. Organomet. Chem. 688 (2003) 168.
[23] R. Boaretto, G. Paolucci, S. Sostero, O. Traverso, J. Mol. Cat. A 204–205 (2003) 253.
[24] C.T. Burns, H. Shen, R.F. Jordan, J. Organomet. Chem. 683 (2003) 240.
[25] T.E. Biterwolf, J.E. Shade, J.E. Brown, W.H. Pearson, Organometallics 14 (1995) 157.
[26] C.M. Alvarez, B. Galan, M.E. Garcia, V. Riera, M.A. Ruiz, Organometallics 22 (2003) 5504.
[27] M.K. Kuimova, W.Z. Alsindi, J. Dyer, D.C. Grills, O.S. Jina, P. Matousek, A.W. Parker, P. Portius, X.Z. Sun, M. Towrie, C. Wilson, J. Yang, M.W. George, Dalton Trans. (2003) 3996.
[28] M. Towrie, D.C. Grills, J. Dyer, J.A. Weinstein, P. Matousek, R. Barton, P.D. Bailey, N. Subramaniam, W.M. Kwok, C. Ma, D. Phillips, A.W. Parker, M.W. George, Appl. Spect. 57 (2003) 367.
[29] J. Dyer, W.J. Blau, C.G. Coates, C.M. Creely, J.D. Gavey, M.W. George, D.C. Grills, S. Hudson, J.M. Kelly, P. Matousek, J.J. McGarvey, Photochem. Photobiol. Sci. 2 (2003) 542.
[30] O.S. Jina, X.Z. Sun, M.W. George, Dalton Trans. (2003) 1773.
[31] F.P.A. Johnson, M.W. George, V.N. Bagratashvili, L.N. Vereshchagina, M. Polikoff, Mendeleev Commun. (1991) 26.
[32] V. Bachler, F.-W. Grevels, K. Kerpen, G. Olbrich, K. Schaffner, Organometallics 22 (2003) 1696.
[33] D.V. Krupenya, E.O. Danilov, M.A.J. Rodgers, S.P. Tunik, J. Phys. Chem. A 107 (2003) 8867.
[34] P.A. Hamley, M.K. Kuimova, A.J. Blake, C. Hughes, S.B.L. Lyons, M. Poliakoff, A.H. Wright, M.W. George, Dalton Trans. (2003) 1545.
[35] R. Krishnan, H.E. Gottlieb, R.H. Schultz, Angew. Chem. 42 (2003) 2179.
[36] H. Kunkely, A. Vogler, Inorg. Chem. Commun. 6 (2003) 830.
[37] H. Kunkely, A. Vogler, Inorg. Chim. Acta 344 (2003) 262.
[38] A.A. Bengali, T.F. Stumbaugh, Dalton Trans. (2003) 354.
[39] S. Gittermann, T. Jiao, T.J. Burkey, Photochem. Photobiol. Sci. 2 (2003) 817.
[40] S. Lugovskoy, J. Lin, R.H. Schultz, Dalton Trans. (2003) 3103.
[41] (a) H. Yang, M.C. Asplund, K.T. Kotz, M.J. Wilkens, H. Frei, C.B. Harris, J. Am. Chem. Soc. 120 (1998) 10154;

(b) H. Yang, K.T. Kotl, M.C. Aspund, C.B. Harris, J. Am. Chem. Soc. 119 (1997) 9564.
[42] (a) L. Andrews, M. Zhou, G.L. Gutsev, J. Phys. Chem. 107 A (2003) 990;
(b) L. Andrews, M. Zhou, G.L. Gutsev, X. Wang, J. Phys. Chem. A 107 (2003) 561.
[43] P.J. Campos, D. Sampedro, M.A. Rodriguez, J. Org. Chem. 68 (2003) 4674.
[44] R.H. Schultz, J. Organomet. Chem. 688 (2003) 1.
[45] (a) D.A. Wink, P.C. Ford, J. Am. Chem. Soc. 107 (1985) 1794;
(b) D.A. Wink, P.C. Ford, J. Am. Chem. Soc. 107 (1985) 5566;
(c) D.A. Wink, P.C. Ford, J. Am. Chem. Soc. 109 (1987) 436.
[46] (a) D.A. Wink, P.C. Ford, J. Am. Chem. Soc. 107 (1985) 1794;
(b) D.A. Wink, P.C. Ford, J. Am. Chem. Soc. 109 (1985) 5566;
(c) D.A. Wink, P.C. Ford, J. Am. Chem. Soc. 109 (1987) 436.
[47] D.R. Tyler, Coord. Chem. Rev. 246 (2003) 291.
[48] E. Schutte, T.J.R. Weakley, D.R. Tyler, J. Am. Chem. Soc. 125 (2003) 10319.
[49] (a) R.M. Noyes, J. Chem. Phys. 22 (1954) 1349;
(b) R.M. Noyes, Prog. React. Kinet. 1 (1961) 129;
(c) R.M. Noyes, J. Am. Chem. Soc. 77 (1955) 2042;
(d) R.M. Noyes, J. Am. Chem. Soc. 78 (1956) 5486.
[50] D. Byun, J.I. Zink, Inorg. Chem. 42 (2003) 4308.
[51] J.C. Green, P. Powell, J.E. van Tilborg, Organometallics 3 (1984) 211.
[52] M.F. Ryan, D.E. Richardson, D.E. Lichtenberger, N.E. Gruhn, Organometallics 13 (1994) 1190.
[53] C.E. Webster, Y. Fan, M.B. Hall, D. Kunz, J.F. Hartwig, J. Am. Chem. Soc. 125 (2003) 858.
[54] (a) K.M. Waltz, J.F. Hartwig, Science 277 (1997) 211;
(b) H. Chen, S. Schlecht, T.C. Semple, J.F. Hartwig, Science 287 (2000) 1995;
(c) K.M. Waltz, J.F. Hartwig, J. Am. Chem. Soc. 122 (2000) 11358.
[55] T.P.M. Goumans, A.W. Ehlers, M.C. van Hemert, R. Rosa, E.-J. Baerends, K. Lammertsma, J. Am. Chem. Soc. 125 (2003) 3558.
[56] T. Akioka, Y. Inoue, A. Yanagawa, M. Hiyamizu, Y. Takagi, A. Sugimori, J. Mol. Cat. A 202 (2003) 31.
[57] F. Wang, D.C. Neckers, J. Org. Chem. 68 (2003) 634.
[58] C. Badarau, Z.Y. Wang, Macromolecules 36 (2003) 6959.
[59] C. Kutal, Coord. Chem. Rev. 211 (2001) 353.
[60] T. Wang, Y.L. Huang, Imaging Sci. J. 51 (2003) 247.
[61] W. Ding, K.A. Johnson, C. Kutal, I.J. Amster, Anal. Chem. 75 (2003) 4624.
[62] J. Dyer, W.J. Blau, C.G. Coates, C.M. Creely, J.D. Gavey, M.W. George, D.C. Grills, S. Hudson, J.M. Kelly, P. Matousek, J.J. McGarvey, J. McMaster, A.W. Parker, M. Towrie, J.A. Weinstein, Photochem. Photobiol. Sci. 2 (2003) 542.
[63] D.M. Dattelbaum, M.K. Itokazu, N.Y.M. Iha, T.J. Meyer, J. Phys. Chem. A 107 (2003) 4092.
[64] M.K. Itokazu, A.S. Polo, N.Y.M. Iha, J. Photochem. Photobiol. A: Chem. 160 (2003) 27.
[65] Y. Hayashi, S. Kita, B.S. Brunschwig, E. Fujita, J. Am. Chem. Soc. 125 (2003) 11976.
[66] H. Hori, Y. Takano, K. Koike, Y. Sasaki, Inorg. Chem. Commun. 6 (2003) 300.
[67] V.W.-W. Yam, K.M.-C. Wong, S.H.-F. Chong, V.C.-Y. Lau, S.C.-F. Lam, L. Zhang, K.-K. Cheung, J. Organomet. Chem. 670 (2003) 205.
[68] S. Zalis, I.R. Farrell, A. Vlcek, J. Am. Chem. Soc. 125 (2003) 4580.
[69] F.W. Vergeer, M.J. Calhorda, P. Matousek, M. Towrie, F. Hartl, Dalton Trans. (2003) 4084.
[70] A.K. Patra, J.M. Rowland, D.S. Marlin, E. Bill, M.M. Olmstead, P.K. Mascharak, Inorg. Chem. 42 (2003) 6812.
[71] C.L. Conrado, J.L. Bourassa, C. Egler, S. Wecksler, P.C. Ford, Inorg. Chem. 42 (2003) 2288.
[72] C.R. Andrew, K.R. Rodgers, R.R. Eady, J. Am. Chem. Soc. 125 (2003) 9548.
[73] D.M. Lawson, C.E.M. Stevenson, C.R. Andrew, R.R. Eady, EMBO J. 19 (2000) 5661.